THE GEOLOGICAL SOCIETY OF AMERICA®

Carbon fluxes from subducted carbonates revealed by uranium excess at Mount Vesuvius, Italy

Riccardo Avanzinelli[1,2*§], Martina Casalini[1*], Tim Elliott[2], and Sandro Conticelli[1,3]
[1]Dipartimento di Scienze della Terra, Università degli Studi di Firenze, Via Giorgio La Pira, 4, I-50121 Florence, Italy
[2]Bristol Isotope Group, School of Earth Sciences, University of Bristol, Queens Road, Bristol BS8 1RJ, UK
[3]Istituto di Geoscienze e Georisorse, Consiglio Nazionale delle Ricerche, Via Giorgio La Pira, 4, I-50121 Florence, Italy

ABSTRACT

The fate of carbonate-rich sediments recycled at destructive plate margins is a key issue for constraining the budget of deep CO_2 supplied to the atmosphere by volcanism. Experimental studies have demonstrated that metasomatic melts can be generated by partial melting of subducted carbonate-pelitic sediments, but signatures of the involvement of such components in erupted magmas are more elusive. We have made new U-Th disequilibria, Sr-Nd-Pb isotope, and high-precision $\delta^{238}U$ analyses on lavas from Mount Vesuvius (Italy) and show that their measured ^{238}U excesses require a mantle source affected by the addition of U-rich carbonated melts, generated by partial melting of subducted calcareous sediments in the presence of residual epidote. Accordingly, we argue that the occurrence of ^{238}U excesses in "sediment-dominated" arc magmas represents diagnostic evidence of addition of carbonate sediments via subduction, hence providing constraints on deep carbon cycling within Earth. Our quantitative enrichment model, combined with published experimental results, allows us to estimate a resulting flux of 0.15–0.8 Mt/yr CO_2 from the subducted carbonates to the mantle source of Mount Vesuvius.

INTRODUCTION

At destructive plate margins, the oceanic slab is subducted into the mantle, carrying both basaltic oceanic crust and overlying sediments. Part of this subducted material is then released at depth, affecting the mantle wedge above the slab, and it is eventually returned to the surface through volcanoes. This flux is a key part of element cycling on Earth (Kelemen and Manning, 2015).

The evidence of this process can be found in the elemental and isotopic compositions of subduction-related magmas worldwide. Globally, the geochemistry of subduction-related volcanic rocks is dictated by the variable contribution of three main components (e.g., Elliott, 2003) (Fig. 1; Fig. DR1 in the GSA Data Repository[1]): (1) the depleted mantle (DM); (2) the slab-derived fluids, with isotope compositions similar to that of subducted basaltic oceanic crust (BOC); (3) the slab-derived melts, with crustal isotope signature, interpreted as deriving from the recycling of subducted sediments.

It can be difficult to deconvolve the contributions of these different components in arc magmas, not least for subducted carbonate-rich sediments. Constraining their involvement is key to directly quantifying the origin of CO_2 emissions from volcanoes, with major consequences for atmospheric fluxes (Burton et al., 2013). Yet their contribution to subduction zone magmas is not necessarily distinctive in many traditionally used geochemical tracers.

Experimental studies (Poli, 2015; Skora et al., 2015) have shown that subducted carbonate-rich sediments (marls) may undergo partial melting if infiltrated by significant amounts of H_2O. The involvement of subducted sedimentary carbonate in the genesis of some subduction-related volcanoes has been suggested on the basis of carbon isotope data on fumaroles and geothermal fluids (van Soest et al., 1998), of minor element contents in olivine (Ammannati et al., 2016), and of whole rock geochemical and isotope data (Conticelli et al., 2015). However, it is commonly difficult to constrain the nature of the recycled sediments from the isotopic compositions of erupted magmas.

Identifying the role of recycled carbonate sediments is further complicated by the possible occurrence of crustal limestone assimilation en route to the surface, which may modify the composition of the erupted magmas, overprinting some of the geochemical and isotopic signatures inherited from the mantle source (e.g., Iacono Marziano et al., 2009).

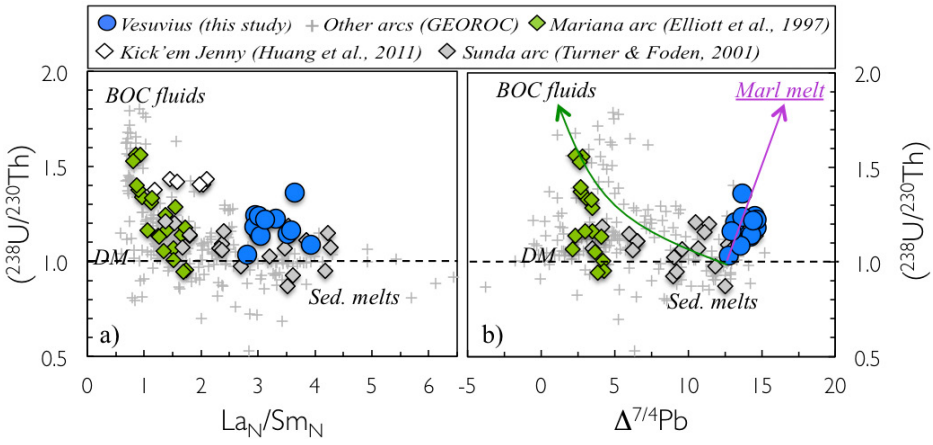

Figure 1. Plot of ($^{238}U/^{230}Th$) (parentheses denoting that the ratio is expressed as activities) versus chondrite-normalized La/Sm (A) and versus $\Delta^{7/4}Pb$ (which represents the difference between the $^{207}Pb/^{204}Pb$ of samples and that of Northern Hemisphere reference line (Hart, 1984) at the sample's $^{206}Pb/^{204}Pb$) (B). Samples from Mount Vesuvius (Italy; this study) are compared with other subduction-related volcanic rocks (data from GEOROC database, http://georoc.mpch-mainz.gwdg.de/georoc/). Samples from Mariana Islands (western North Pacific Ocean; Elliott et al., 1997; Avanzinelli et al., 2012) are representative of typical oceanic arc with variable contributions of sediment (sed.) melt relative to basaltic oceanic crust (BOC) fluids. Data for Kick'em Jenny (Caribbean; Huang et al., 2011) and Sunda arc (Indonesia; Turner and Foden, 2001) are representative of sediment-dominated arc lavas with possible contribution from carbonate-rich sediments. Depleted mantle is assumed to have ($^{238}U/^{230}Th$) = 1 and $\Delta^{7/4}Pb$ = 0. Full data set for Mount Vesuvius samples is provided in the Data Repository (Tables DR1–DR4 [see footnote 1])

*Both authors contributed equally to the paper
§E-mail: riccardo.avanzinelli@unifi.it
[1]GSA Data Repository item 2018073, analytical methods, modeling description (including Figures DR1–DR4), and data tables (Tables DR1–DR7), is available online at http://www.geosociety.org/datarepository/2018/ or on request from editing@geosociety.org.

In this study, we report the occurrence of marked ^{238}U excesses at Mount Vesuvius (Italy), and coupling these ^{230}Th-^{238}U measurements with variations in $\delta^{238}U$ (the parts-per-thousand difference in $^{238}U/^{235}U$ relative to a reference solution standard, CRM145) and radiogenic isotope data (Sr, Nd, and Pb), we demonstrate the involvement of deep-recycled carbonate-rich lithologies in the mantle source of these magmas.

Uranium-series disequilibria in arc lavas have long been used to constrain the contribution of slab-derived liquids (fluids and/or melts), as well as the time scales of their transfer from the slab to the surface (e.g., Gill and Condomines, 1992; for further details, see the Data Repository). "Fluid-dominated" arcs are generally characterized by significant ^{238}U excess over ^{230}Th, that is, $(^{238}U/^{230}Th) > 1$ (Fig. 1), a feature classically attributed either to the higher fluid mobility of U with respect to Th (e.g., Gill and Condomines, 1992), or to the presence of residual accessory phases preferentially retaining Th during melting of the subducting basaltic oceanic crust (Avanzinelli et al., 2012). Sediment melts, on the contrary, seem to impart either no disequilibrium (Condomines and Sigmarsson, 1993) or minor ^{230}Th excesses (Avanzinelli et al., 2012) to the erupted lavas.

^{238}U EXCESS AT MOUNT VESUVIUS AS TRACER FOR SUBDUCTION-DERIVED CARBONATE-RICH SEDIMENT MELTS

Mount Vesuvius lavas have significant ^{238}U excesses (Voltaggio et al., 2004; Avanzinelli et al., 2008) (Fig. 1), which may suggest the involvement of BOC-derived fluids along the lines of the general processes proposed for arc magmas (Elliott, 2003).

Yet, when compared to the global arc database (Fig. 1), the observed ^{238}U excesses in Vesuvius lavas are anomalous. Indeed, the geochemical and Sr-Nd-Pb isotopic compositions of Vesuvius lavas invariably lie at the "sediment-dominated" end of the global arc trend (Fig. 1; Fig. DR1), suggesting a mantle source strongly enriched by sediment-derived melts. In this scenario, the contribution from BOC-derived fluids should be obscured by the sediment-melt signal, due to the greater capacity of the latter as an incompatible trace-element carrier with respect to hydrous fluids.

Vesuvius lavas therefore are anomalous among subduction-related magmas. Yet, the occurrence of ^{238}U excesses in sediment-dominated arc magmas is not a unique characteristic of Vesuvius (Fig. 1), but also occurs in a few other cases such as in the Lesser Antilles (e.g., Kick'em Jenny volcano; Huang et al., 2011), Nicaragua (Reagan et al., 1994), and part of the Sunda arc (e.g., Tambora and Sangeang Api volcanoes in Indonesia; Turner and Foden, 2001).

Given the sediment-derived trace element and long-lived isotope characteristics (i.e., Sr, Nd and Pb; Fig. 1; Fig. DR1; Tables DR1–DR4 in the Data Repository) of Vesuvius lavas, the occurrence of large ^{238}U excesses requires either extremely large amounts of BOC-derived fluids, to remain evident against the sediment contribution, or the addition of a sedimentary component recently enriched in U with respect to Th. When plotted against radiogenic isotope ratios such as $^{87}Sr/^{86}Sr$ (Fig. DR3) and $\Delta^{7/4}Pb$ (Hart, 1984; Fig. 1), Vesuvius lavas do not show a decrease of $\Delta^{7/4}Pb$ with increasing $(^{238}U/^{230}Th)$ as would be expected if the ^{238}U excess was due to BOC-derived fluids. Instead, the samples characterized by larger ^{238}U excesses show similar or higher $\Delta^{7/4}Pb$ (and $^{87}Sr/^{86}Sr$) compared to samples close to secular equilibrium. Hence, the component responsible for the ^{238}U excess at Mount Vesuvius also imparts a crustal signature to the magmas, indicating it must derive from subducted sediments.

To further constrain the origin of the U-rich component, we made high-precision $\delta^{238}U$ measurements. Natural variations in $^{238}U/^{235}U$ are linked to the partial reduction of hexavalent U(VI) to tetravalent U(IV) (see the review in Andersen et al., 2017) and are limited to the low-temperature environment of Earth's surface, so that the $^{238}U/^{235}U$ signatures of magmas provide a robust tracer of near-surface–processed U. A recent study (Andersen et al., 2015) reported data for the Mariana arc, showing a clear trend from isotopically heavy U composition in sediment-dominated islands to isotopically light values in fluid-dominated ones. This feature, which is associated with the shift from ^{230}Th to ^{238}U excesses in erupted magmas (Fig. 2), has been interpreted to result from the isotopically light composition of U-rich fluids originating from the upper, most-altered portion of the BOC.

The Mount Vesuvius lavas measured in this study show instead an invariably heavy U isotopic composition, thus excluding a major role for fluids from the most altered portion of the BOC. Even considering the heavier $\delta^{238}U$ reported for the bulk BOC (Andersen et al., 2015), exceedingly large amount of fluids would be required to generate the composition of Vesuvius lavas (Fig. 2). Coupled with the radiogenic isotope data (Fig. 1; Fig. DR3), these observations clearly indicate the need for a sediment-derived, isotopically heavy, U-rich component.

Thus, we analyzed the $\delta^{238}U$ of a suite of Italian sediments that represent a likely analogue of the subducted sedimentary lithologies beneath Mount Vesuvius (Table DR4). This also includes a Mesozoic limestone of the type that forms the country rock hosting the magma chamber of Mount Vesuvius, which can be used to evaluate the effect of limestone assimilation that has been claimed to play a major role in controlling the magma compositions (Iacono Marziano et al., 2009). The Mesozoic limestone shows an extremely low $\delta^{238}U$ (Fig. 2; Table DR4),

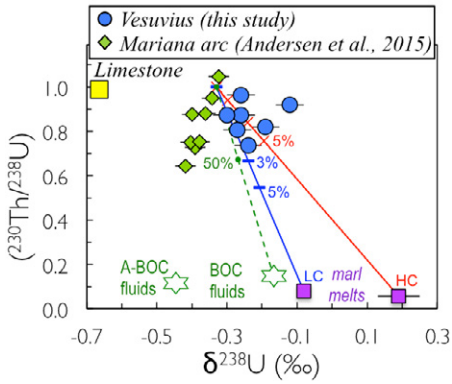

Figure 2. Plot of $(^{230}Th/^{238}U)$ versus $\delta^{238}U$. Averages between replicate analyses are plotted when available (Table DR4 in the Data Repository [see footnote 1]); error bars are based on reproducibility (2σ) of international rock standards (Table DR4), and for $(^{230}Th/^{238}U)$ are smaller than symbol size; standard errors (2 s.e.) for single measurements are reported in Table DR4. Data for Mariana Islands (western North Pacific Ocean; Andersen et al., 2015) are reported for comparison along with estimated composition of altered (A-BOC) and bulk basaltic oceanic crust (BOC) (Andersen et al., 2015). Mixing lines between mantle (assumed in secular equilibrium) and two possible sediment-melt components from high-carbonate (HC) and low-carbonate (LC) marls are reported. Mixing model with BOC-derived fluids is also shown. Mesozoic limestone sample (yellow square) is representative of wall-rock carbonate hosting Mount Vesuvius magma chamber. Details of model parameters are provided in Data Repository; compositions of all end members are reported in Table DR5.

indicating that the amount of U added to the magmas through limestone assimilation must be negligible. The same conclusion can be obtained from the subhorizontal alignment of the data on an U-Th isochron diagram. This does not exclude the occurrence of significant limestone assimilation at Mount Vesuvius (~10%; Iacono Marziano et al., 2009) affecting some of the features of the magmas (e.g., major elements). In terms of U-Th disequilibria, however, this process may be responsible for some of the vertical scattering shown by the data on the U-Th isochron diagram (Fig. DR2), but not for the ^{238}U excess (see details in the Data Repository).

On the contrary, the two carbonate-rich clays (i.e., marlstones) that we analyzed show high $\delta^{238}U$, making them suitable candidates to provide the distinctive signature of the studied magmas. The involvement of recycled carbonate-rich sediments as a "marl melt component" (MMC) can provide the solution to explain the ^{238}U excess at Mount Vesuvius. A recent experimental study (Skora et al., 2015) showed that the abundances of some key trace elements in melts from calcareous sediments (i.e., marls) at subarc pressure-temperature (*P-T*) conditions are controlled by epidote, that it is stabilized during melting and can remain as a residual phase

until relatively high temperatures (900 °C). Epidote hosts limited amounts of U and Th, but it preferentially retains Th over U. Hence melts generated from carbonate-rich sediment in the presence of residual epidote have ^{238}U excess, but at the same time they remain enriched in both Th and U. Natural evidence of the same process can be found in the composition of melt inclusions hosted in the deeply subducted carbonate rocks of the Kokchetav massif (northern Kazakhstan; $P = 4.5–6.0$ GPa; $T \sim 1000$ °C), which show extreme U/Th ratios (>2; Korsakov and Hermann, 2006).

Therefore, melting of isotopically heavy, carbonate-rich pelitic sediments could produce suitable metasomatic agents to impart both the high $\delta^{238}U$ and the ^{238}U excess observed in Vesuvius lavas. In Figure 2, we modeled this process (see also Fig. DR3 and details in the Data Repository, and Table DR5), showing that <5% of such a component is sufficient to impart U-series disequilibrium in a mantle source that had been previously strongly metasomatized, as evident from the radiogenic isotope composition of the samples with the smallest ^{238}U excess (Fig. 1).

Evidence for such a process is not restricted to Mount Vesuvius. Other subduction-related magmas with sediment-dominated geochemical and radiogenic isotope signatures show significant ^{238}U excess (e.g., Kick'em Jenny; Huang et al. 2011; Fig. 1). Therefore, we suggest that the presence of significant ^{238}U excesses in enriched (i.e., sediment-dominated) subduction-related rocks may represent key evidence for the involvement of carbonate-rich subducted sediments.

This has important implications for constraining the carbon budget emissions at arcs. A recent study (Mason et al., 2017) suggested that shallow remobilization of crustal carbon (i.e., assimilation) may dominate the volcanic arc emissions over the deeper "subduction" carbon cycle, reporting Mount Vesuvius as one of the main locations where CO_2 is mainly derived from interaction with the shallow crust (see also Iacono-Marziano et al., 2009). Our data indicate instead that subducted carbonate-rich sediment melts (MMC) have an important role in the chemical and isotopic composition of Vesuvius lavas, and Italian magmatism more generally (e.g., Avanzinelli et al., 2008; Conticelli et al., 2015), resulting in significant "subduction-derived" CO_2 fluxes (see also Frezzotti et al., 2009).

MMC-DERIVED CO_2 FLUXES

We attempted to estimate the MMC-derived fluxes by combining the two-step mantle enrichment model used to explain the ^{238}U excess of Vesuvius lavas with published parameters regarding the output rates of Mount Vesuvius and the amount of CO_2 carried along with the MMC.

The rationale of our calculation is that, given the extreme incompatibility of U both during mantle melting and magma differentiation (Blundy and Wood, 2003), it can be assumed that the total amount of U in Vesuvius magmatic products is the same as that hosted in their mantle source. Hence, knowing the magmatic output rates of Mount Vesuvius and the average U contents of the erupted products, it is possible to calculate the U flux from the mantle source. Combining this estimate with the U concentration calculated for the metasomatized mantle source in our two-step mantle enrichment model, we estimated the mass flux of mantle undergoing melting. Finally, we extrapolated the mass flux of MMC added to the mantle source of Mount Vesuvius from the proportion of MMC required to generate the observed average ($^{230}Th/^{238}U$) of Vesuvius lavas (Table DR5). This can be converted to MMC-derived CO_2 fluxes simply by estimating the amount of CO_2 carried along with the MMC. Given the large uncertainties in several of the parameters used for the calculation—namely, (1) the U content of the erupted magmas, (2) the output rates, (3) the U and the CO_2 content of the MMC, and (4) the amount of MMC required to produce the mean ^{238}U excess observed in Vesuvius magmas—we performed Monte Carlo simulations, letting the four aforementioned parameters randomly vary between maximum and minimum values. Further details on the various parameters used are provided in the Data Repository and in Tables DR6 and DR7 therein. The results (Fig. 3) of our calculation yield average MMC-derived CO_2 fluxes between ~0.15 Mt/yr and ~0.8 Mt/yr.

It is important to stress that the estimated fluxes presented in our study account only for the CO_2 derived from the addition of the MMC and do not consider other possible sources of CO_2 that contribute to the total CO_2 fluxes released at Mount Vesuvius, such as those related to the shallow assimilation of limestone and those added from the subducted slab during the first step of mantle enrichment. Also, they represent an estimated CO_2 flux averaged over the whole investigated period (A.D. 1697–1944), which would increase considerably (almost double) if considering only the active phases of the volcano (Scandone et al., 2008; see the Data Repository), and conversely decrease in low-activity phases. Therefore, it is difficult to compare our estimates with CO_2 emissions from presently active volcanoes. Keeping this in mind, the range of MMC-derived CO_2 fluxes calculated for Mount Vesuvius is comparable to fluxes calculated from present-day emission at arc volcanoes, such as Stromboli (southern Italy; 0.73 Mt/yr; Burton et al., 2013) and Montserrat (Lesser Antilles; 0.56 Mt/yr; Burton et al., 2013). This suggests that CO_2 fluxes deriving from subducted carbonate-rich material are significant for the total carbon budget emitted at some arc volcanoes. Mount Vesuvius is not active at present, hence direct measurements of volcanic CO_2 fluxes are not available, although estimates based on the isotopic composition of groundwater (Caliro et al., 2005) and diffuse soil degassing (Frondini et al., 2004) report values of ~0.1 Mt/yr, which are lower than those indicated by our calculation. In addition, it must be taken into account that a significant portion of the present-day CO_2 emitted around Mount Vesuvius has been linked to limestone assimilation (Iacono Marziano et al., 2009).

Yet, the ^{238}U excesses of Vesuvius magmas, when combined with $\delta^{238}U$ and Pb, Sr, and Nd isotope ratios, can only be explained by the addition in their source of carbonate-rich sediment melts that contributes significantly to the CO_2 fluxes released at the surface, especially during the more-active phases of the volcano.

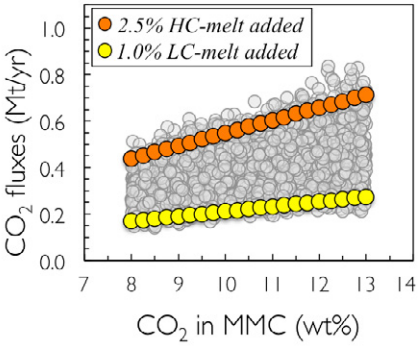

Figure 3. Calculated marl melt component (MMC)–derived CO_2 fluxes plotted versus CO_2 content of U-rich MMC used for each simulation (see text and Data Repository [see footnote 1] for further details). Gray circles represent all results of Monte Carlo simulations performed by letting main parameters used for calculation vary between minimum and maximum (see Table DR7); orange and yellow circles represent results obtained by keeping constant U concentration in erupted magmas (U_{ves} = 6.5 ppm) and output rate (OR = 3.5 × 10^6 m^3/yr) in two case scenarios assuming 2.5% addition of high-carbonate (HC) and 1.0% addition of low-carbonate (LC) component (see Tables DR5 and DR6), respectively.

ACKNOWLEDGMENTS

We thank F. Aliberti, M. Andersen, A. Bragagni, E. Braschi, C. Coath, R. Cioni, M. Mattei, J. Prytulak, S. Tommasini, and M. Ulivi for discussions and help on various aspects of the paper. Comments by J. Foden, A. Skelton, S. Turner, F. Gaillard, and an anonymous reviewer, and careful editorial handling by J.B. Murphy, greatly improved the manuscript. Avanzinelli was funded by a Marie Curie postdoctoral fellowship (025136-OIBH2O) and by the MIUR (Ministero dell'Istruzione dell'Università e della Ricerca) "Rientro dei Cervelli" program. Funding for this research was also provided by Progetti di Ricerca di Interesse Nazionale grants 2010TT22SC_001, 20158A9CBM, and 2015EC9PJ5.

REFERENCES CITED

Ammannati, E., Jacob, D.E., Avanzinelli, R., Foley, S.R., and Conticelli, S., 2016, Low Ni olivine in silica-undersaturated ultrapotassic igneous rocks as evidence for carbonate metasomatism in the mantle: Earth and Planetary Science Letters,

v. 444, p. 64–74, https://doi.org/10.1016/j.epsl.2016.03.039.
Andersen, M.B., Elliott, T., Freymuth, H., Sims, K.W.W., Niu, Y., and Kelley, K.A., 2015, The terrestrial uranium isotope cycle: Nature, v. 517, p. 356–359, https://doi.org/10.1038/nature14062.
Andersen, M.B., Stirling, C.H., and Weyer, S., 2017, Uranium isotope fractionation, *in* Teng, F.Z., et al., eds., Non-Traditional Stable Isotopes: Mineralogical Society of America Reviews in Mineralogy and Geochemistry 82, p. 799–850, https://doi.org/10.1515/9783110545630-020.
Avanzinelli, R., Elliott, T., Tommasini, S., and Conticelli, S., 2008, Constraints on the genesis of the potassium-rich Italian volcanics from U/Th disequilibrium: Journal of Petrology, v. 49, p. 195–223, https://doi.org/10.1093/petrology/egm076.
Avanzinelli, R., Prytulak, J., Skora, S., Heumann, A., Koetsier, G., and Elliott, T., 2012, Combined ^{238}U-^{230}Th and ^{235}U-^{231}Pa constraints on the transport of slab-derived material beneath the Mariana Island: Geochimica et Cosmochimica Acta, v. 92, p. 308–328, https://doi.org/10.1016/j.gca.2012.06.020.
Blundy, J., and Wood, B., 2003, Mineral-melt partitioning of uranium, thorium and their daughters, *in* Bourdon, B., et al., eds., Uranium-Series Geochemistry: Mineralogical Society of America Reviews in Mineralogy and Geochemistry 52, p. 59–123, https://doi.org/10.2113/0520059.
Burton, M.R., Sawyer, G.M., and Granieri, D., 2013, Deep carbon emissions from volcanoes, *in* Hazen, R.M, et al., eds., Carbon in Earth: Mineralogical Society of America Reviews in Mineralogy and Geochemistry 75, p. 323–354, https://doi.org/10.2138/rmg.2013.75.11.
Caliro, S., Chiodini, G., Avino, R., Cardellini, C., and Frondini, F., 2005, Volcanic degassing at Somma-Vesuvio (Italy) inferred by chemical and isotopic signatures of groundwater: Applied Geochemistry, v. 20, p. 1060–1076, https://doi.org/10.1016/j.apgeochem.2005.02.002.
Condomines, M., and Sigmarsson, O., 1993, Why are so many magmas close to ^{238}U-^{230}Th radioactive equilibrium?: Geochimica et Cosmochimica Acta, v. 57, p. 4491–4497, https://doi.org/10.1016/0016-7037(93)90498-L.
Conticelli, S., Avanzinelli, R., Ammannati, E., and Casalini, M., 2015, The role of carbon from recycled sediments in the origin of ultrapotassic igneous rocks in the Central Mediterranean: Lithos, v. 232, p. 174–196, https://doi.org/10.1016/j.lithos.2015.07.002.
Elliott, T., 2003, Tracers of the slab, *in* Eiler, J., ed., Inside the Subduction Factory: American Geophysical Union Geophysical Monograph 138, p. 23–45, https://doi.org/10.1029/138GM03.
Elliott, T., Plank, T., Zindler, A., White, W., and Bourdon, B., 1997, Element transport from slab to volcanic front at the Mariana arc: Journal of Geophysical Research, v. 102, p. 14,991–15,019, https://doi.org/10.1029/97JB00788.
Frezzotti, M.L., Peccerillo, A., and Panza, G., 2009, Carbonate metasomatism and CO_2 lithosphere-asthenosphere degassing beneath the Western Mediterranean: An integrated model arising from petrological and geophysical data: Chemical Geology, v. 262, p. 108–120, https://doi.org/10.1016/j.chemgeo.2009.02.015.
Frondini, F., Chiodini, G., Caliro, S., Cardellini, C., and Granieri, D., 2004, Diffuse CO_2 soil degassing at Vesuvio, Italy: Bulletin of Volcanology, v. 66, p. 642–651, https://doi.org/10.1007/s00445-004-0346-x.
Gill, J.B., and Condomines, M., 1992, Short-lived radioactivity and magma genesis: Science, v. 257, p. 1368–1376, https://doi.org/10.1126/science.257.5075.1368.
Hart, S.R., 1984, A large-scale isotope anomaly in the Southern Hemisphere mantle: Nature, v. 309, p. 753–757, https://doi.org/10.1038/309753a0.
Huang, F., Lundstrom, C.C., Sigurdsson, H., and Zhang, Z., 2011, U-series disequilibria in Kick'em Jenny submarine volcano lavas: A new view of timescales of magmatism in convergent margins: Geochimica et Cosmochimica Acta, v. 75, p. 195–212, https://doi.org/10.1016/j.gca.2010.05.036.
Iacono-Marziano, G., Gaillard, F., Scaillet, B., Pichavant, M., and Chiodini, G., 2009, Role of non-mantle CO_2 in the dynamics of volcano degassing: The Mount Vesuvius example: Geology, v. 37, p. 319–322, https://doi.org/10.1130/G25446A.1.
Kelemen, P.B., and Manning, C.E., 2015, Reevaluating carbon fluxes in subduction zones, what goes down, mostly comes up: Proceedings of the National Academy of Sciences of the United States of America, v. 112, p. E3997–E4006, https://doi.org/10.1073/pnas.1507889112.
Korsakov, A.V., and Hermann, J., 2006, Silicate and carbonate melt inclusions associated with diamonds in deeply subducted carbonate rocks: Earth and Planetary Science Letters, v. 241, p. 104–118, https://doi.org/10.1016/j.epsl.2005.10.037.
Mason, E., Edmonds, M., and Turchyn, A.V., 2017, Remobilization of crustal carbon may dominate volcanic arc emissions: Science, v. 357, p. 290–294, https://doi.org/10.1126/science.aan5049.
Poli, S., 2015, Carbon mobilized at shallow depths in subduction zones by carbonatitic liquids: Nature Geoscience, v. 8, p. 633–636, https://doi.org/10.1038/ngeo2464.
Reagan, M.K., Morris, J.D., Herrstrom, E.A., and Murrell, M.T., 1994, Uranium series and beryllium isotope evidence for an extended history of subduction modification of the mantle below Nicaragua: Geochimica et Cosmochimica Acta, v. 58, p. 4199–4212, https://doi.org/10.1016/0016-7037(94)90273-9.
Scandone, R., Giacomelli, L., and Speranza, F., 2008, Persistent activity and violent strombolian eruptions at Vesuvius between 1631 and 1944: Journal of Volcanology and Geothermal Research, v. 170, p. 167–180, https://doi.org/10.1016/j.jvolgeores.2007.09.014.
Skora, S., Blundy, J.D., Brooker, R.A., Green, E.C.R., de Hoog, J.C.M., and Connolly, J.A.D., 2015, Hydrous phase relations and trace element partitioning behaviour in calcareous sediments at subduction-zone conditions: Journal of Petrology, v. 56, p. 953–980, https://doi.org/10.1093/petrology/egv024.
Turner, S., and Foden, J., 2001, U, Th and Ra disequilibria, Sr, Nd and Pb isotope and trace element variations in Sunda arc lavas: Predominance of a subducted sediment component: Contributions to Mineralogy and Petrology, v. 142, p. 43–57, https://doi.org/10.1007/s004100100271.
van Soest, M.C., Hilton, D.R., and Kreulen, R., 1998, Tracing crustal and slab contributions to arc magmatism in the Lesser Antilles island arc using helium and carbon relationships in geothermal fluids: Geochimica et Cosmochimica Acta, v. 62, p. 3323–3335, https://doi.org/10.1016/S0016-7037(98)00241-5.
Voltaggio, M., Branca, M., Teduesco, D., Tuccimei, P., and Di Pietro, L., 2004, ^{226}Ra-excess during the 1631–1944 activity period of Vesuvius (Italy): A model of alpha-recoil enrichment in a metasomatized mantle and implications on the current state of the magmatic system: Geochimica et Cosmochimica Acta, v. 68, p. 167–181, https://doi.org/10.1016/S0016-7037(03)00236-9.

Manuscript received 2 October 2017
Revised manuscript received 11 December 2017
Manuscript accepted 13 December 2017

Printed in USA

GSA Data Repository 2018073 DOI:10.1130/G39766.1

Carbon fluxes from subducted carbonates revealed by uranium excess at Mount Vesuvius, Italy

Riccardo Avanzinelli, Martina Casalini, Tim Elliott, Sandro Conticelli

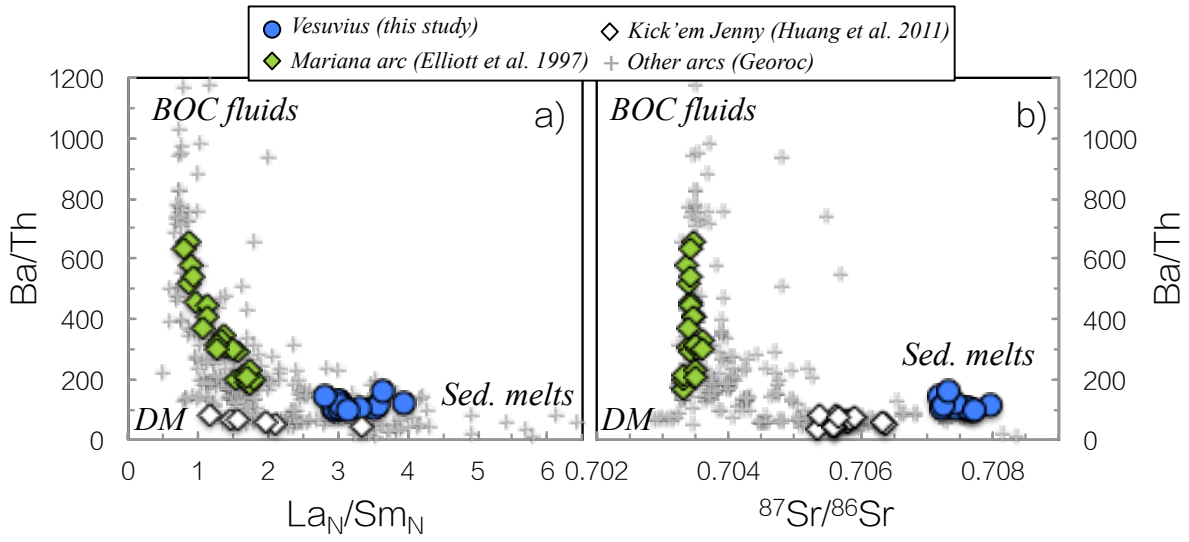

Fig. DR1*. Plot of chondrite-normalized La/Sm and $^{87}Sr/^{86}Sr$ vs. Ba/Th. The samples from Vesuvius fall on the 'sediment-dominated' part (i.e. high La_N/Sm_N and $^{87}Sr/^{86}Sr$, but low Ba/Th), indicating with a mantle enriched by the addition of melts from subducted sedimentary material.*

SAMPLE SELECTION AND ANALYTICAL METHODS.

Thirteen samples of Vesuvius volcanic rocks (lava flows and scoria), erupted from medieval period (AD 472 – AD 1631) to AD 1944, were selected for this study. In addition few sedimentary carbonate-rich rocks from Apennines were also analyzed and used as a proxy for recycled sediments. Apennines are made up of Tethyan sedimentary sequences scraped off and piled up onto the continental margin during Tethys closure (Treves, 1984). Sample SD 48 and SD 11 are marlstones with variable $CaCO_3$ (SD 48: High-Carbonate, hereafter HC; SD 11: Low Carbonate, hereafter LC) outcropping within the Northern Apennines (Conticelli et al., 2015) whilst sample ERN 57 (Boari et al, 2009a) is a Mesozoic limestone that is representative of the carbonate-platform hosting Vesuvius magma chamber (Del Moro et al., 2001; Iacono Marziano et al., 2009).

Samples were powdered and analyzed for major, trace elements and Sr-Nd-Pb isotopes. ^{230}Th-^{238}U disequilibria were measured in Vesuvius samples; given their age sediments were assumed in secular equilibrium and not measured. A subset of ten samples (including the 3 sediments) was selected for the analysis of $^{238}U/^{235}U$.

The whole dataset is provided in tables DR1-4, where further details on the analytical procedures are also reported along with accuracy and reproducibility values based on replicate analyses of international rock standards, as well as further information on the analytical protocols (Avanzinelli et al., 2005, 2014; Hoffman et al., 2007; Andersen et al., 2014; Hiess et al., 2012).

^{230}Th-^{238}U DISEQUILIBRIA.

Uranium series isotopes are short-lived, highly incompatible nuclides that are formed by the decay of long-lived ^{238}U and ^{235}U, with ^{230}Th being the short-lived daughter of ^{238}U with a half-life of ~75kyr. The nuclides of each decay chain evolve to a state of "secular equilibrium" with their parents, such that their activities (rates of atomic disintegrations, denoted by round brackets) are equal, which means (^{230}Th/^{238}U) = 1. Disequilibrium can be by fractionation between U and Th, yielding (^{230}Th/^{238}U) ≠ 1 with either ^{238}U- or ^{230}Th-excess; if the system remains closed, secular equilibrium is then restored in~ 5 half lives of the daughter nuclide (375kyr for ^{230}Th).

For these reasons 'undisturbed' mantle sources (e.g. those within-plate and mid oceanic ridge settings) are considered in secular equilibrium, whilst in subduction-related environment the slab-derived components may preferentially introduce U or Th to the mantle wedge, hence producing disequilibria (e.g., Hawkesworth et al., 1993). Despite the similar and highly incompatible character of U and Th in most mineral phases, there are several processes that can produce ^{238}U-^{230}Th disequilibria, mostly relating to the mechanism of mantle melting and to the geodynamic setting in which magmas are generated (see thorough reviews in Bourdon and Turner, 2003).

MORBs and within-plate magmas generally show ^{230}Th excess that are explained with the in-growth of ^{230}Th during adiabatic mantle melting (e.g., Elliott, 1997). The scenario is more complex in in subduction-related settings, where magmas show variable (^{230}Th/^{238}U) that are generally related to the nature of the slab-derived component affecting the mantle wedge (i.e., BOC-fluids vs. sediment melts: Fig. 1; e.g., Elliott, 2003). Large ^{238}U-excesses are common in depleted arc lavas and are interpreted as a consequence of aqueous fluid-addition from the altered, mafic oceanic crust (e.g.), due to the higher U in the aqueous fluid phase, with respect to Th. Other authors suggest to that ^{238}U are related to the presence of residual accessory phases, such as allanite (Klimm et al., 2008) preferentially retaining Th during melting of the subducting basaltic oceanic crust (Avanzinelli et al., 2012).

Sediment-dominated, enriched arcs lavas are more variable: a general decrease of ^{238}U-excess with increasing Th concentrations in arc lavas (e.g., Condomines and Sigmarrsson, 1993; Hawkesworth et al., 1997) has suggested that sediment melts are added either close to secular equilibrium or that enough time has elapsed since melting that any initial disequilibrium has decayed (Elliott et al., 1997). More recently it has been shown that arc magmas can preserve the ^{230}Th-excesses generated during sediment melting (Avanzinelli et al., 2012) due to the preferable retention of U in garnet.

Shallow processes during magma ascent, differentiation and storage in the crust may also affect the U-series composition of the magmas: fractional crystallisation becomes important mostly in the later stages of magma differentiation, due to the highly incompatible behavior of both U and Th in all the major early crystallizing phases (e.g. Blundy & Wood, 2003); crustal contamination is instead believed to drive the composition of the magmas back towards secular equilibrium (Reubi et al., 2011).

Our model assumes that the ^{238}U-excess, as well as δ^{238}U and Sr-Nd-Pb isotope ratios measured in the erupted products of Vesuvius are the same of those of their mantle source. This assumption implies that the U-Th disequilibria of Vesuvius lavas ware not modified during mantle melting and magma differentiation and storage. The effects of these processes on the composition of the erupted products and the possible implication for the suggested model are discussed hereafter.

Limestone Assimilation

Several authors (Iacono Marziano et al., 2009; Dallai et al., 2011; Pichavant et al., 2014) have suggested a prominent role for assimilation of limestone affecting both the composition of the erupted magmas and the CO_2 emissions. Other studies have provided evidence for an important role of carbonate-rich sediments melts added via subduction to the mantle source of many southern Italian volcanoes (e.g., Peccerillo, 1985; Conticelli and Peccerillo, 1992; Avanzinelli et al., 2008; Frezzotti et al., 2009; Conticelli et al., 2015; Ammannati et al., 2016). The main evidence for this process is the high enrichment in incompatible trace elements of the erupted magmas, both at Vesuvius and in other volcanoes in southern Italy. Such an enrichment cannot be generated by limestone assimilation, which instead should dilute (if any) the incompatible trace element contents in the magmas. A limited trace-element exchange between the host limestone and the magmas was also confirmed by a study on crustal xenoltihs from Vesuvius (Del Moro et al., 2001)

This does not exclude the possibility of the two processes (i.e., limestone assimilation and addition of subduction-related recycling of carbonate-rich sediment melts to the mantle source of the Vesuvius magmas) may coexist (e.g., Boari et al., 2009b). For the purpose of this study it is important to evaluate to what extent the assimilation of wall-rock limestone have affected the U elemental and isotopic composition Vesuvius magmas, and thus whether or not it can be responsible for the ^{238}U-excess that are used here as evidence of the deeper addition of carbonate-rich sediment melts to the mantle wedge.

In order to evaluate the effect of such a process on both (^{230}Th/^{238}U) and ^{238}U/^{235}U of Vesuvius magmas we measured δ^{238}U of one sample of Mesozoic limestone (ERN 57) belonging to the carbonate platform that constitute the country rocks hosting the Vesuvius magma chamber. This sample shows an extremely light U isotope composition (δ^{238}U = -0.67 ‰) opposite to the shift from mantle towards higher δ^{238}U shown by Vesuvius samples.

Limestone hosts significantly more U than Th, resulting in high U/Th and developing over time extremely high (^{230}Th/^{232}Th) (Fig. DR 3). As an example, assuming secular equilibrium, sample ERN 57 has (^{238}U/^{232}Th) = (^{230}Th/^{232}Th) = 6.85; the same holds true considering a limestone sample erupted as xenolith within the 1944 eruption of Vesuvius (sample C-5 and C-3 from Del Moro et al., 2001) having (^{238}U/^{232}Th) = (^{230}Th/^{232}Th) > 14.

Vesuvius samples have both (^{238}U/^{232}Th) and (^{230}Th/^{232}Th) significantly lower than limestone, with (^{238}U/^{232}Th) ranging from 0.91 to 1.21 and a smaller variation in (^{230}Th/^{232}Th), from 0.96 to 1.07, resulting in variable ^{238}U-excesses that define a quasi-horizontal trend in the classic equiline diagram (Fig. DR2). It is difficult to asses whether assimilation would involve partial or total melting of the host limestone, and, in the first case, whether wall-rock partial melting would produce fractionation between U and Th (hence producing U or Th excesses); in either case, the assimilated material would invariably have extremely high (^{230}Th/^{232}Th), hence producing a significant effect on the (^{230}Th/^{232}Th) of the contaminated magmas. In the figure the bulk assimilation of such high (^{238}U/^{232}Th) and (^{230}Th/^{232}Th) is modeled starting from both the sample with both the smallest and largest ^{238}U-excess, in order to evaluate whether such a process could be responsible for the isotope variation observed at Vesuvius. Figure DR2 clearly shows that the assimilation of limestone, even at the higher extent suggested for Vesuvius (up to of 10-15%: Iacono Marziano et al. 2009), could produce some of the scattering shown by the dataset, but it cannot be responsible for the horizontal displacement of the samples toward high (^{238}U/^{232}Th) and thus toward the observed ^{238}U-excess.

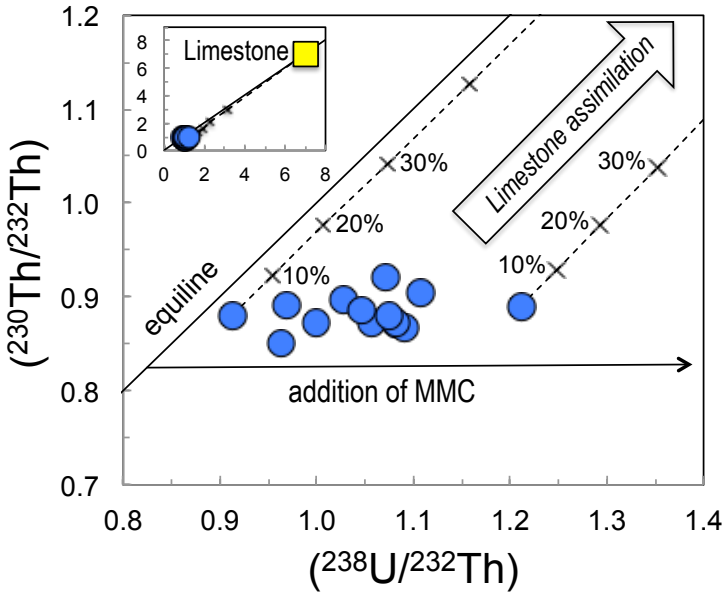

***Fig. DR2**. Effect of wall-rock limestone assimilation on the U-series activity ratios of Vesuvius volcanic rocks. Dotted lines represent bulk mixing of Mesozoic limestone ERN 57 with the two magmas with the highest and lowest ^{238}U-excess. The isotope composition of the wall rock limestone (shown in the inset) is calculated from its U and Th content (Table DR1) assuming secular equilibrium. For comparison un-metamorphosed limestone xenoliths erupted within 1944 (Dal Moro et al., 2001) yield recalculated (^{238}U/^{232}Th) = (^{230}Th/^{232}Th) varying from 15 to 105. Error bars are smaller than the symbols.*

Fractional crystallization and mantle melting

As stated above, fractional crystallization has also little effect on both U and Th due to their similar and high incompatibility in the main crystallizing phases, unless significant amounts of U- or Th-rich phases (e.g., apatite) are fractionated. At Vesuvius no correlation is observed between ^{238}U-excess and any fractionation index (e.g., MgO) including those sensitive to apatite fractionation (i.e., P_2O_5).

Mantle melting may affect (^{230}Th/^{238}U) according to time-dependent melting models (e.g., Elliott, 1997) that have been applied to subduction-related magmatism (e.g., Thomas et al., 2002; Avanzinelli et al., 2012). The net effect of melting on ^{230}Th-^{238}U is to decrease the extent ^{238}U-excess in the erupted magmas with respect to the original value of their mantle source, due to the time-dependent ingrowth of ^{230}Th during melting (Avanzinelli et al., 2012; Elliott, 1997; Thomas et al., 2002; Zou and Zindler, 2000). A detailed quantification of this process is beyond the purpose of this study and will require additional data on other U-series parent-daughter disequilibria (such as ^{231}Pa-^{235}U). Accounting for the possible effect of mantle melting would require to infer a slightly greater initial ^{238}U-excess in the mantle source; this would consequently require a larger addition of U-rich MMC, eventually resulting in slightly larger estimates of CO_2 fluxes than those estimated (Fig. 3). On the other hand, the 'ingrowth' effect on ^{230}Th-^{238}U disequilibria of arc magmas is generally small with respect to other parent daughter pairs (Avanzinelli et al., 2012), as confirmed by the near equilibrium composition of many arcs (Condomines and Sigmarsson, 1993). Considering this, CO_2 fluxes calculated by our model (see details below) might be slightly under-estimated, although we believed that the potential effect of such a process should be smaller than the uncertainty of some used parameters, which is accounted for in our Monte Carlo simulation (Fig. 3., details in the calculations are provided below).

MODELLING THE MANTLE SOURCE OF VESUVIUS MAGMAS.

Vesuvius magmas are invariably characterized by radiogenic Sr and Pb and unradiogenic Nd isotope composition, indicating a crustal component within their mantle source, regardless of the extent of the U-series disequilibria (Figs. 1, DR1). Therefore, we adopted a two-step enrichment model: i) a first enrichment capable of producing the composition of the lavas with no ^{238}U-excess; ii) a second step accounting for the addition of the Marl Melt Component (i.e., MMC) and thus the ^{238}U-excess.

For this first step we applied mixing models using the end-members compositions of mantle wedge (i.e., MW) and slab-derived component (i.e., SC) reported for the neighboring Stromboli volcano (Tommasini et al., 2007) (Table DR5). Stromboli and Vesuvius volcanic products show several similarities in terms of geochemical and isotopic composition (Fig. DR3) suggesting a common (or similar) mantle source (Peccerillo, 2001). The lack of ^{238}U-excess at Stromboli (Tommasini et al., 2007) indicates, however, that Stromboli magmas must originate from a mantle source not affected by the contribution of the U-rich MMC.

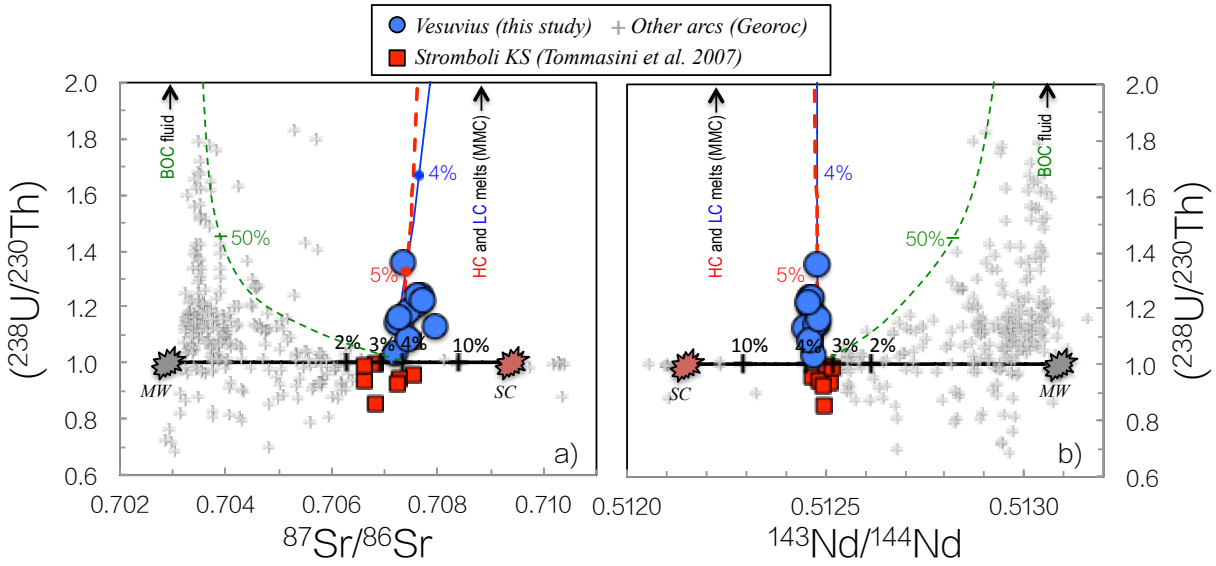

***Fig. DR3**. Two-step mixing between process. The green, red and blue mixing curves are calculated between a mantle source enriched with 3.5% of SC (step I – Table DR5) and the BOC fluid, the HC and the LC melt, respectively (Step II: Table DR5). HC and LC melts represent two possible compositions of the U-rich Marl-Melt Component (MMC) starting from sediment samples SD 48 (High-Carbonate marl, HC) and SD 11 (Low-Carbonate marl, LC). Samples from Stromboli are reported as red squares.*

Both MW and SC (Table DR5) were assumed having secular equilibrium (^{230}Th/^{238}U) and δ^{238}U equal to the bulk-earth average (i.e., -0.33 ‰: Andersen et al., 2015). From this calculation we estimated a mantle enriched by an average of 3.5 % SC as a starting point to model the second step (Fig. DR3, Table DR5).

In the second step we modeled the addition of the MMC into the previously enriched (Step I) mantle. The geochemical and isotopic composition of the two possible U-rich MMCs shown in figure 2 (and Fig. DR3) were calculated starting from the two marl sediments measured in this study (Tables DR1-4) and modeling sediment melting according to the experiments of Skora et al. (2015) (Table DR5). For each sediment sample we used the melting parameters reported for similar lithologies (HC for SD 48 and LC for SD 11). We chose run conditions characterized by the presence of residual epidote (in order to produce the enrichment in U over Th in the resulting melts) and by the complete exhaustion of phengite (which would have retained K and Rb, resulting in a depletion of such elements not observed in the data). The temperatures of the experimental runs (850-900°C) are slightly higher than those estimated at the slab/mantle interface by thermal models of both 'cold' subduction (e.g., Peacock, 2003: Kelemen et al., 2003). This can be explained, for example assuming the physical incorporation of portions of the subducted sediments into the mantle, by imbrication, as melanges or via diapirs (e.g., Kelemen et al., 2003: Gerya et al., 2006, Nielsen and Marshall, 2017), and their melting at higher temperatures (Fig. DR4).

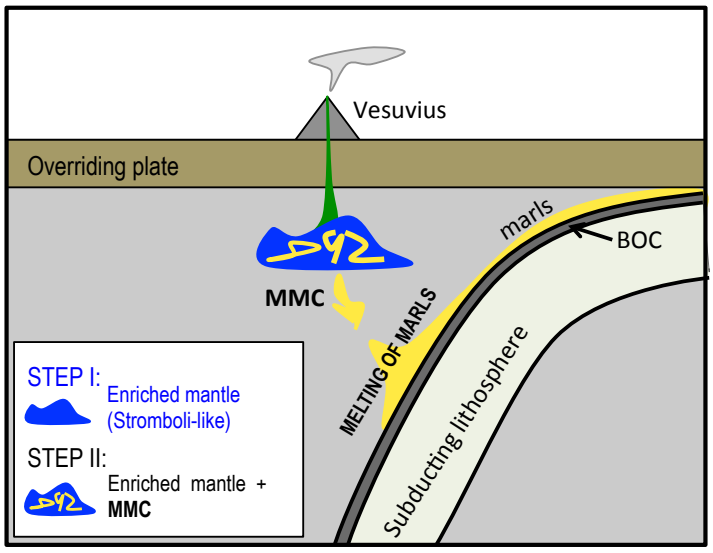

Fig. DR4*. Simplified illustration of the two-step enrichment process operating under Vesuvius. Melting of subducted marls (with residual epidote) generates the MMC that reacts (Step II) with a previously enriched (Step I) mantle, hence imparting the observed ^{238}U-excess to the mantle source of Vesuvius. The MMC-enriched mantle source then undergoes melting to generates Vesuvius magmas*

The composition of the BOC fluid used in figures 2 and DR3 (from Avanzinelli et al. 2012, Andersen et al., 2015) is also reported in Table DR5. It is worth stressing that the correlation between U-Th disequilibria and both δ^{238}U and Sr-Nd-Pb isotopes is not as good as it would be expected for a simple two end-members mixing model. This suggests that the marl melt component (MMC) is not isotopically homogeneous, hence it may derive from several isotopically different starting sediments undergoing subduction and melting. Moreover, the U/Th of the sediment melt is dictated by the phase relations during melting, and it is not inherited from the original down-going sediment.

Most of the data in figure 2 and DR3 can be reproduced by the addition of the two proposed MMC components. Other samples show higher δ^{238}U and ^{87}Sr/^{86}Sr, suggesting the involvement of a component with slightly different isotope composition. Regardless of this complexity, our data clearly shows that the ^{238}U-excess observed at Vesuvius can be obtained only through the addition of sediment-melt component, and cannot be due to addition of BOC fluid-like agents as it occurs in more typical island arc settings (e.g., Marianas).

The mixing models performed in this study are therefore used to provide an estimate, as good as possible, of the amount of MMC recycled into the mantle source of Vesuvius, especially for constraining the U mass balance that will be used in the next section in the attempt of quantifying CO_2 fluxes. The key parameters in this calculation are the U content and U/Th of the modeled MMC, whilst its Sr-Nd-Pb isotope composition and δ^{238}U, has no effect on the results.

The experimental study of Skora et al. (2015) shows that melts produced by carbonate-rich sediments in the presence of residual epidote have higher Ba/Th than those produced by carbonate-poor epidote-free lithologies. Ba/Th of Vesuvius is lower with respect to 'fluid-dominated' arcs (Fig. DR1), but it is higher than that of other Italian potassic rocks (Avanzinelli et al., 2008) and Stromboli. In fact, the slight increase of Ba/Th from the values observed in the potassic rocks of Stromboli (i.e., Ba/Th = 80-95: Tommasini et al., 2007) - which are considered here as representative of the first step of subduction-related mantle enrichment - to the higher values of Vesuvius rocks (i.e., Ba/Th = 92-140, Table DR1) is consistent with the further addition of the MMC, in the two-step process suggested in this study. These melts, would then react with the previously metasomatised mantle wedge along the lines of the process described in detail in Ammannati et al (2016).

ESTIMATING MMC-DERIVED CO_2 FLUXES.

Since the U-rich MMC is released by recycled sedimentary carbonates, we attempted to constrain how much of its CO_2 was released during subduction and thus the flux of MMC-derived CO_2 affecting the mantle source of the magmas. This is an extremely complex task, due to the large number of variables that affect the calculation and are difficult to constrain.

MMC derived CO_2 fluxes ($f_{CO2\text{-}MMC}$) was calculated as follows:

$$f_{CO2-MMC} = f_{MMC} \times [CO_2]_{MMC} \quad (1)$$

where $[CO_2]_{MMC}$ is the amount of CO_2 carried with the MMC (in wt%) and f_{MMC} is the mass flux (Mt/yr) of MMC into the mantle source of Vesuvius over the investigated period, that is:

$$f_{MMC} = f_{MS} \times \%MMC \quad (2)$$

where *%MMC* is the proportion (as wt%) of MMC required to produce the observed U-excess, extrapolated from the two-step mixing model and f_{MS} is the mass flux of mantle source undergoing melting, and thus producing magmas. The latter (i.e., f_{MS}) was calculated by mass balancing U as

$$f_{MS} = \frac{fU_{MS}}{[U]_{MS}} \quad (3)$$

where $[U]_{MS}$ is the average concentration of U in the mantle source calculated through the two-step enrichment model described above, and fU_{MS} is, that is the total mass of U involved in the melting process (partitioned between the melt and the residue) divided by the considered period of activity (A.D. 1697 – 1944), that is the mass flux of U from the mantle source.

Considering the extreme incompatibility of U both during mantle melting and magma differentiation (Blundy and Wood, 2003), it can be assumed that all the U has been completely partitioned in the magmas and then in the erupted products (i.e., negligible U is lost in the residual mantle or fractionated by crystallized mineral phases). This means that all the U hosted in the mantle source is directly transferred to the erupted magmas, hence fU_{MS} is equal to the mass flux U erupted (fU_{ER}), which in turn can be calculated as:

$$fU_{MS} = fU_{ER} = [U]_{ER} \times OR_{1697-1944} \quad (4)$$

where $[U_{ER}]$ is the average concentration of U in the erupted products and $OR_{1697\text{-}1944}$ is the output rate in Mt/yr estimated for Vesuvius during the 1697-1944 period (Cortini and Scandone, 1982; Scandone et al., 1986; Santacroce et al., 1993; Scandone et al., 2008: generally published values are available as volume/year).

Merging these four simple relations, the MMC-derived CO_2 fluxes can be expressed as:

$$f_{CO2-MMC} = \left\{\left[\frac{([U]_{ER} \times OR_{1697-1944})}{[U]_{MS}}\right] \times \%MMC\right\} \times [CO_2]_{MMC} \quad (5)$$

The parameters involved in the calculation are extremely difficult to constrain and even the best estimate of them may carry large uncertainty. In order to account for this large variability we performed Monte Carlo simulation letting all the parameters varying between a maximum and a minimum value.

The results of our Monte Carlo simulation are shown in figure 3 and yields $f_{CO2\text{-}MMC}$ between 0.2 and 0.8 Mt/yr. The ranges used for each parameter are reported in Table DR7, and are discussed in more details hereafter.

CO_2 contents of the MCC: $[CO2]_{MMC}$.

The study of Skora et al. (2015) reports the CO_2 content of the starting sedimentary materials, but unfortunately does not provide its concentration (or estimates of it) in the sediment melts, also due

to the occurrence of *fish eggs* testifying the presence of a coexisting fluid phase which was not measured. The paper however, provides the final phase proportion, for each experiment, including the amount of residual carbonate and melt generated.

Starting from the initial CO_2 contents and the phase proportions, we calculated the amount of CO_2 lost during the experiments, by assuming that all the CO_2 retained in the residue was hosted within the carbonate phase. The amount of retained CO_2 was then calculated by simply allotting it into the carbonate using stoichiometric estimation. The remaining amount of CO_2 (i.e., the portion lost during the melting experiment) was then redistributed into the fraction of melt produced during the experiment, so to calculate a wt% value. This is obviously a simplification, since it does not account for the mass of the coexisting liquid phase, which means implicitly assuming to be negligible with respect to that of the melt.

The application of this approach for the starting sediments of Skora et al. (2015) yields ~8 and ~9 wt% of CO_2 released during the partial melts of the Low-Carbonate (LC) and High-carbonate (HC) lithologies, respectively (Table DR6). The somewhat surprisingly similar values are explained by the smaller amount of residual carbonate in the experiment involving the carbonate-poor lithology, so that almost all of its CO_2 is released during the melting experiment, whilst during the experiments performed with the carbonate-rich lithology a significant part of CO_2 is retained in the residue.

The two Italian marlstones, SD 48 and SD 11 used in our calculation are very similar in bulk composition to the carbonate-rich (HC) and carbonate-poor (LC) lithology used by Skora et al. (2015), respectively. Initial CO_2 contents of SD 48 and SD 11 are not available and it is also difficult to assess their phase proportion during melting; assuming the same CO_2/LOI ratio and phase proportion of the respective HC and LC of Skora et al. (2015), the amount of CO_2 carried with the sediment melt would be ~12 wt% for SD 48 and ~9 wt% for SD 11 (Table DR6).

Whether the suggested amount of CO_2 is dissolved in the melts or carried as a separate fluid or gas phase is difficult to constrain, since it is related to the solubility of CO_2 in the melt which depends in turn on several parameters (e.g., pressure, amount of dissolved water, f_{CO2}, and melt composition, e.g., Ni and Keppler, 2013). Considering that the total mass of such fluid or gas phase should be negligible with respect to that of the sediment melt, aforementioned values were assumed as the wt% amount of CO_2 carried along with the U-rich MMC, regardless of the physical form in which it is transferred.

According to the considerations made above we used a possible range of CO_2 contents for the MMC between 8 and 13 wt.%.

%MMC, $[U]_{ER,}$ and *$[U]_{MS.}$*

For any U isotope composition, the enrichment model allows to calculate the amount of MMC required (*%MMC)* and the resulting U content in the mantle source ($[U]_{MS}$). Excluding three medieval samples (AD 472 - AD 1631), for which is more difficult to find estimates of output rates (see hereafter), our dataset includes volcanic products from AD 1697 to AD 1944, with U concentrations ($[U]_{ER}$) ranging from 5.7 and 7.5 ppm (i.e., similar to the overall variation reported on Georoc for the same periods of activity).

These samples have mean ($^{230}Th/^{238}U$) ~ 0.86 that are best reproduced with the addition of ~ 2.5 of the HC or ~ 1.0% of the LC sediment melt, respectively (Table DR5). In the two-step melting model adopted, the aforementioned additions of MMC produce a metasomatised mantle source with almost identical U content, ~ 0.28 to 0.29 ppm (Table DR5), due to the higher initial concentration in the LC starting sediment (SD 11).

Output rates: $OR_{1697-1944}$

Santacroce et al. (1993) calculated output fluxes of 3.5-4-0 x 10^6 m^3/yr for the AD 1872 - AD 1906 activity and similar values (i.e., 3.9 x 10^6 m^3/yr) were suggested by Scandone et al. (1986) from AD 1906 to AD 1944., A more recent study (Scandone et al., 2008) investigated in detail the volcanic activity of Vesuvius from AD 1638 and AD 1944, providing estimates of the supply rates of several eruptions as well as the duration of the refilling process. From those estimates it is possible to calculating the total mass of magma supplied to the system and to redistribute it through the 306 year-span, resulting in a mean supply rate of 3.0 x 10^6 m^3/yr, similar to the previous estimates.

According to these estimates the MMC-derived CO_2 fluxes were calculated with output rates ranging between 3.0 x 10^6 m^3/yr and 4.0 x 10^6 m^3/yr, yielding a total range of possible values between ~ 0.2 Mt/yr and ~ 0.8 (Fig. 3).

It is important to stress that, however, in the study of Scandone et al. (2008) the time accounted by the supplying periods adds up to cover only ~ 140 of the total 306 year-span. This indicate that magma arrival in the system is not a continuous process, but it occurs in phases of high, yet variable, supply rate alternated with periods with no magma supplied to the system. Accordingly it was suggested a mean supply rate for the 'active' periods of ~ 5.7 x 10^6 m^3/yr (Scandone et al., 2008), which is significantly higher than the values reported above. In terms of CO_2 fluxes, this would convert in 'active' periods with average MMC-derived fluxes between 0.7 and 1.2 Mt/yr (depending on the CO_2 content of MCC) alternated by periods with negligible MCC derived CO_2.

Comparison with directly measured CO_2 fluxes.

The present day emissions of CO_2 at Vesuvius, ~ 0.1 Mt/yr (i.e., 300t/day: Caliro et al., 2005, Frondini et al., 2004, Iacono Marziano et al., 2009) estimated from the isotopic composition of groundwater (Caliro et al., 2005) and diffused soil degassing (Frondini et al., 2004), are lower than those indicated by our calculation.

This is not surprising if considering what discussed in the previous section. At present Vesuvius shows no sign of significant input of magma in the systems, and also the release of magmatic CO_2 may be limited by the lack of an open conduit system, which might instead being present during the AD 1631 - AD 1944 period (Scandone et al., 2008). On the other hand it must be taken into account that a significant portion of the present day-emission at Vesuvius might be due to the interaction between the magma and the limestone in the shallow crust (Iacono Marziano et al., 2009; Dallai et al., 2011; Pichavant et al., 2014). In addition, it must be considered that much larger fluxes are suggested for the whole Campanian area (~ 3 Mt/yr Chiodini et al., 2004). Considering the presence in the Campanian area of other volcanoes, such as Ischia and the Phlegrean Fields, that have erupted significant volumes of products showing 'sediment-dominated' isotope compositions with ^{238}U-excess (Avanzinelli et al., 2008), we suggest that the MMC-derived CO_2 fluxes may represent a significant, portion of the total CO_2 budget of the area.

An interesting datum against which to compare our estimates of MMC-derived CO_2 fluxes is the present-day mean plume CO_2 flux measured at Stromboli (i.e., 0.73 Mt/yr: Burton et al., 2013). Stromboli is a presently active, open-conduit volcano, characterized by a style of activity and output fluxes (Marsella et al., 2012) comparable to that of Vesuvius from AD 1631 to AD 1944 (Scandone et al., 2008) and with no evidence of shallow interaction with carbonates. Also, the mantle source of Stromboli is similar to that of Vesuvius, except for the lack of the U-rich MMC. Assuming that the CO_2 flux measured at Stromboli may represent a proxy for the first step of mantle enrichment also at Vesuvius, we can argue that the MMC-derived fluxes at Vesuvius may account for a significant portion (up to half according to our calculation) of its deep (i.e., mantle derived) CO_2.

ADDITIONAL REFERENCES

Andersen, M.B., Romaniello, S., Vance, D., Little, S.H., Herdman, R., and Lyons, T.W.A, 2014, Modern framework for the interpretation of $^{238}U/^{235}U$ in studies of ancient ocean redox: Earth and Planetary Science Letters, v. 400, p. 184–194.

Avanzinelli, R., Boari, E., Conticelli, S., Francalanci, L., Guarnieri, L., Perini, G., Petrone, C. M., Tommasini, S., and Ulivi, M., 2005, High precision Sr, Nd, and Pb isotopic analyses using new generation thermal ionisation mass spectrometer: aims and perspective for isotope geology applications: Periodico di Mineralogia, v. 74, p. 147–166.

Avanzinelli, R., Braschi, E., Marchionni, S., and Bindi, L., 2014, Mantle melting in within-plate continental settings: Sr–Nd–Pb and U-series isotope constraints in alkali basalts from the Sicily Channel (Pantelleria and Linosa Islands, Southern Italy): Lithos, v. 188, p. 113–129.

Baker, J., Peate, D., Waight, T., and Meyzen, C., 2004, Pb isotopic analysis of standards and samples using a ^{207}Pb-^{204}Pb double spike and thallium to correct for mass bias with a double-focusing MC-ICP-MS: Chemical Geology, v. 211, p. 275–303.

Boari, E., Tommasini, S., Laurenzi, M.A., and Conticelli, S., 2009a, Transition from ultrapotassic kamafugitic to sub-alkaline magmas: Sr, Nd, and Pb isotope, trace element and ^{40}Ar–^{39}Ar age data from the Middle Latin Valley volcanic field, Roman Magmatic Province, Central Italy: Journal of Petrology, v. 50, p. 1327–1357.

Boari, E., Avanzinelli, R., Melluso, L., Giordano, G., Mattei, M., De Benedetti, A., Morra, V., and Conticelli, S., 2009b, Isotope geochemistry (Sr–Nd–Pb) of leucite-bearing volcanic rocks from 'Colli Albani' volcano, Roman Magmatic Province, Central Italy: inferences on volcano evolution and magma genesis: Bulletin of Volcanology v. 71, p. 977–1005.

Bourdon, B., Henderson, G.M., Lundstrom, C.C., and Turner, S.P., eds., 2003. Uranium-Series Geochemistry: Reviews in Mineralogy and Geochemistry v. 52, 656pp.

Conticelli, S., and Peccerillo, A., 1992. Petrology and geochemistry of potassic and ultrapotassic volcanism in central Italy: petrogenesis and inferences on the evolution of the mantle sources: Lithos v. 28, p. 221-240.

Cortini, M., and Scandone, R., 1982, The feeding system of Vesuvius between 1754 and 1944: Journal of Volcanology and Geothermal Research, v. 12, p. 393–400.

Dallai, L., Cioni, R., Boschi, C., and D'Oriano, C., 2011, Carbonate derived CO_2 purging magma at depth: influence on the eruptive activity of Somma-Vesuvius, Italy: Earth and Planetary Science Letters, v. 310, p. 84–95.

Del Moro, A., Fulignati, P., Marianelli, P., and Sbrana, A., 2001, Magma contamination by direct wall-rock interaction: constraints from xenoliths from the walls of a carbonate-hosted magma chamber (Vesuvius 1944 eruption): Journal of Volcanology and Geothermal Research, v. 112, p. 15–24.

Elliott, T., 1997, Fractionation of U and Th during mantle melting: a reprise: Chemical Geology, v. 139, p. 165–183.

Gerya, T.V., Connolly, J.A.D., Yuen, D.A., Gorczyk, W., and Capel, A.M. 2006, Seismic implications of mantle wedge plumes: Physics of the Earth and Planetary Interiors v. 156, p. 59–74.

Hawkesworth, C.J., Gallagher, K., Hergt, J.M. and McDermott F., 1993, Mantle and slab contributions in arc magmas: Annual Review Earth and Planetary Science, v. 21, p. 175-204.

Hawkesworth, C.J., Turner, S.P., Peate, D.W., McDermott, F. and van Calsteren, P., 1997, U-Th isotopes in arc magmas: implications for element transfer from the subducted crust: Science v. 276, p. 551-555.

Hiess, J., Condon, D.J., McLean, N., and Noble, S.R., 2012, $^{238}U/^{235}U$ Systematics in Terrestrial Uranium-Bearing Minerals: Science v. 335, p. 1610–1614.

Hoffmann, D., Prytulak, J., Richards, D., Elliott, T., Coath, C.D., Smart, P.L., and Scholz, D., 2007, Procedures for accurate U and Th isotope measurements by high precision MC–ICPMS: International Journal of Mass Spectrometry, v. 264, p. 97–109.

Kelemen, P.B., Rilling, J.L., Parmentier, E.M., Mehl, L., and Hacker, B.R., 2003, Thermal structure due to solid-state flow in the mantle wedge beneath arcs, *in* Eiler, J., and Hirschmann M., eds., Inside the Subduction Factory: American Geophysical union Monograph series v. 138, 293– 311.

Klimm, K., Blundy, J.D., and Green, T.H., 2008, Trace element partitioning and accessory phase saturation during H_2O-saturated melting of basalt with implications for subduction zone chemical fluxes: Journal of Petrology, v. 49, p. 523–553.

Marsella, M., Baldi, P., Coltelli, M., and Fabris, M., 2012, The morphological evolution of the Sciara del Fuoco since 1868: reconstructing the effusive activity at Stromboli volcano: Bulletin of Volcanology, v. 74, p. 231–248.

Ni, H.W., and Keppler, H., 2013, Carbon in silicate melts: *in* Hazen, R.M, Jones, A.P., and Baross, J.A., eds., Carbon in Earth: Review in Mineralogy and Geochemistry, v. 75, p. 251–287.

Nielsen, S.G. and Marshall, H.R., 2017. Geochemical evidence for mélange melting in global arcs: Science Advance v. 3, e1602402.

Peacock, S.M. 2003. Thermal structure and metamorphic evolution of subducting slab: *in* Eiler, J., and Hirschmann M., eds., Inside the Subduction Factory: American Geophysical union Monograph series v. 138, p. 293– 311.

Peccerillo, A., 1985, Roman comagmatic province (Central Italy); evidence for subduction-related magma genesis: Geology v. 13, p. 103–106.

Peccerillo, A., 2001, Geochemical similarities between the Vesuvius, Phlegraean Fields and Stromboli Volcanoes: petrogenetic, geodynamic and volcanological implications: Mineralogy and Petrology, v. 73, p. 93–105.

Pichavant, M., Scaillet, M., Pommier, A., Iacono-Marziano, G., and Cioni, R., 2014, Nature and evolution of primitive Vesuvius magmas: an experimental study: Journal of Petrology, v. 55, p. 2281-2310.

Reubi, O., Bourdon, B., Dungan, M.A., Koornneef, J.M., Selles, D., Langmuir, C.H., and Aciego, S., 2011, Assimilation of the plutonic roots of the Andean arc controls variations in U-series disequilibria at Volcan Llaima, Chile: Earth and Planetary Science Letters, v. 303, p. 37–47.

Santacroce, R., Bertagnini, A., Civetta, L., Landi, P., and Sbrana, A., 1993, Eruptive dynamics and petrogenetic processes in a very shallow magma reservoir: the 1906 eruption of Vesuvius: Journal of Petrology, v. 34, p. 383–425.

Scandone, R., Iannone, F. and Mastrolorenzo, G., 1986, Stima dei parametri dinamici dell'eruzione del 1944 del Vesuvio: Bollettino IGNV 1986, p. 487–512.

Tommasini, S., Heumann, A., Avanzinelli, R., and Francalanci, L., 2007, The fate of high angle dipping slabs in the subduction factory: an integrated trace element and radiogenic isotope (U, Th, Sr, Nd, Pb) study of Stromboli volcano, Aeolian Arc, Italy: Journal of Petrology, v. 48, p. 2407–2430.

Treves, B., 1984, Orogenic belts as accretionary prisms: the example of the Northern Apennines: Ofioliti, v. 9, p. 577–618.

Thirlwall, M.F., 1991, Long-term reproducibility of multicollector Sr and Nd isotope ratio analysis: Chemical Geology, v. 94, p. 85–104.

Thomas, R.B., Hirschmann, M.M., Cheng, H., Reagan, M.K., and Edwards, R.L., 2002, ($^{231}Pa/^{235}U$)–($^{230}Th/^{238}U$) of young mafic volcanic rocks from Nicaragua and Costa Rica and

the influence of flux melting on U-series systematics of arc lavas: Geochimica et Cosmochimica Acta, v. 66, p. 4287-4309.

Weis, D., Kieffer, B., Maerschalk, C., Barling, J., de Jong, J., Williams,G.A., Hanano, D., Pretorius, W., Mattielli, N., Scoates, J.S., Goolaerts, A., Friedman, R.M., and Mahoney, J.B., 2006, High precision isotopic characterization of USGS reference materials by TIMS and MC-ICPMS: Geochemistry Geophysics Geosystems, v. 7, Q08006.

Zou, H., and Zindler, A., 2000, Theoretical studies of ^{238}U–^{230}Th–^{226}Ra and ^{235}U–^{231}Pa disequilibria in young lavas produced by mantle melting: Geochimica et Cosmochimica Acta, v. 64, p. 1809–1817.

Table DR 1. Eruption date, type, location, major and trace element composition of Vesuvius and Sediment samples

Vesuvius

Sample name	Eruption date	type	Latitude	Longitude	ref.	SiO2 wt%	TiO2 wt%	Al2O3 wt%	Fe2O3 wt%	FeO wt%	MnO wt%	MgO wt%	CaO wt%	Na2O wt%	K2O wt%	P2O5 wt%	LOI wt%	Sum wt%	Mg-V
VES 01	1697 A.D.	Lava Flow	40.7639°N	14.3711°E	this study	47.74	1.03	17.22	8.60	*	0.15	4.49	9.95	2.40	7.39	0.98	0.32	100.3	54.9
VES 02	1794 A.D.	Bomb	40.8114°N	14.3911°E	this study	48.22	1.00	16.79	8.70	*	0.16	4.79	10.21	2.28	6.89	0.89	0.34	100.3	56.2
VES 05	1861 A.D.	Lava Flow	40.8053°N	14.3872°E	this study	47.65	1.01	17.71	8.79	*	0.16	4.04	9.27	2.65	7.56	0.92	0.40	100.2	51.7
VES 06	1861 A.D.	Scoria	40.8000°N	14.3844°E	this study	46.96	1.08	17.25	8.91	*	0.16	4.52	9.95	2.75	6.98	0.94	0.87	100.4	54.2
VES 07	1737 A.D.	Lava Flow	40.7981°N	14.3975°E	this study	47.43	0.98	17.59	8.68	*	0.16	3.96	9.20	2.53	7.64	0.87	0.46	99.5	51.5
VES 09	1760 A.D.	Lava Flow	40.7767°N	14.4241°E	this study	47.97	0.95	17.35	8.24	*	0.15	4.18	9.04	2.90	8.02	0.83	0.59	100.2	54.2
VES 11	1754 A.D.	Lava Flow	40.7819°N	14.4717°E	this study	48.43	0.98	17.14	8.35	*	0.15	4.72	9.68	2.61	6.88	0.89	0.26	100.1	56.8
VES 16	1929 A.D.	Lava Flow	40.8131°N	14.4669°E	this study	47.92	1.01	16.94	8.94	*	0.16	4.80	10.59	2.31	6.64	0.89	0.28	100.5	55.6
VES 17	*1944 A.D*	*Lava Flow*	40.8317°N	14.4119°E	*Avanzinelli et al., 2008*	*48.75*	*1.03*	*19.29*	*1.10*	*6.70*	*0.16*	*3.71*	*8.44*	*1.54*	*8.22*	*0.84*	*0.24*	*100.0*	*50.3*
VES 18	*1858 A.D.*	*Lava Flow*	40.8236°N	14.3867°E	*Avanzinelli et al., 2008*	*49.45*	*0.91*	*19.36*	*2.54*	*5.18*	*0.15*	*3.02*	*8.26*	*1.58*	*8.27*	*0.70*	*0.59*	*100.0*	*45.9*
95VS131	*472-1631 A.D.*	*Scoria*	40.8122°N	14.4614°E	*Avanzinelli et al., 2008*	*48.18*	*1.14*	*16.33*	*9.56*	*	*0.17*	*4.48*	*9.62*	*2.49*	*6.93*	*0.82*	*0.28*	*100.0*	*52.2*
97VS718b	*472-1631 A.D.*	*Scoria*	40.7791°N	14.4347°E	*Avanzinelli et al., 2008*	*48.47*	*0.99*	*13.71*	*7.77*	*	*0.14*	*7.45*	*12.28*	*1.87*	*5.67*	*0.75*	*0.89*	*100.0*	*69.1*
95VS135	*472-1631 A.D.*	*Scoria*	40.8122°N	14.4614°E	*Avanzinelli et al., 2008*	*48.66*	*1.07*	*16.30*	*9.18*	*	*0.16*	*4.36*	*8.91*	*2.68*	*7.52*	*0.76*	*0.40*	*100.0*	*52.5*

new data from Actlabs Laboratories, Ontario (Canada)

Sample name	Sc ppm	V ppm	Cr ppm	Co ppm	Ni ppm	Cu ppm	Zn ppm	Ga ppm
VES 01	17	265	< 20	27	30	100	60	18
VES 02	22	261	50	27	30	110	70	18
VES 05	16	262	20	27	30	110	70	19
VES 06	19	256	30	27	20	100	70	19
VES 07	17	258	20	28		110	70	20
VES 09	16	235	40	25	30	90	80	18
VES 11	21	238	40	25	30	90	60	17
VES 16	23	268	30	27		110	70	18
VES 17	*	*230*	*	*23*	*26*	*101*	*	*15*
VES 18	*	*194*	*	*21*	*19*	*99*	*	*15*
95VS131	*	*268*	*30*	*26*	*33*	*112*	*	*16*
97VS718b	*	*228*	*218*	*26*	*66*	*68*	*	*12*
95VS135	*	*242*	*48*	*25*	*28*	*119*	*	*15*

ICP-MS trace elements data: Actlabs Ontario (Canada)

Sediments

Sample name	Lithology	ref	SiO2 wt%	TiO2 wt%	Al2O3 wt%	Fe2O3 wt%	FeO wt%	MnO wt%	MgO wt%	CaO wt%	Na2O wt%	K2O wt%	P2O5 wt%	LOI wt%	Sum wt%	Mg-V
SD 11	Carbonate-poor marlstone	this study	57.39	0.44	11.15	3.25	*	0.07	2.84	10.55	1.86	1.96	*	10.50	100.0	0.6
SD 48	Carbonate-rich marlstone	this study	23.88	0.29	6.45	2.25	*	0.09	1.45	34.15	0.60	1.19	*	29.66	100.0	0.6
ERN57	*Mesozoic Limestone*	*Boari et al. (2009)*	*7.66*	*0.07*	*2.09*	*0.76*	*	*0.03*	*1.05*	*47.59*	*0.55*	*0.28*	*0.08*	*39.85*	*100.0*	*0.7*

ICP-MS trace elements data: new data performed at Bristol Isotope Group (BIG)

Sample name	Sc ppm	V ppm	Cr ppm	Co ppm	Ni ppm	Cu ppm	Zn ppm	Ga ppm
SD 11	7.4	*	*	6.1	43.0	6.1	142	10.1
SD 48	5.4	*	*	9.4	48.0	64.5	300	9.0
ERN57	*1.2*	*17*	*	*1.9*	*	*3.10*	*14.7*	*

Quality Control: *Meas/Ref is the ratio between the measured concentration value and the certified one of a number (n) of rock standards measured together with the samples*

	SiO2	TiO2	Al2O3	Fe2O3	FeO	MnO	MgO	CaO	Na2O	K2O	P2O5
Meas/Cert	*1.00*	*1.01*	*1.01*	*1.00*	*	*0.98*	*0.98*	*1.00*	*1.00*	*0.95*	*0.93*
1 σ	*0.01*	*0.04*	*0.04*	*0.02*	*	*0.07*	*0.05*	*0.02*	*0.04*	*0.13*	*0.17*
#	*14*	*14*	*14*	*14*	*	*13*	*14*	*14*	*14*	*14*	*14*

	Sc	V	Cr	Co	Ni	Cu	Zn	Ga
Meas/Cert	*1.01*	*1.04*	*0.92*	*0.98*	*0.98*	*1.02*	*0.98*	*1.04*
1 σ	*0.06*	*0.05*	*0.10*	*0.07*	*0.10*	*0.09*	*0.16*	*0.11*
#	*12*	*12*	*18*	*27*	*18*	*28*	*27*	*19*

Major and minor element contents were measured by XRF and AAS at Università degli Studi di Firenze. Further trace element data were acquired at Activation Laboratories (Ancaster, Ontario) via Fusion ICPMS. The trace element contents of the three sediment samples were determined through ICPMS (Thermo Finnigan Element 2) at the Bristol Isotope Group laboratories (hereafter BIG) of the University of Bristol (UK). Reproducibility of International Standards is expressed as 1σ; (#) = number of analyses.

Table DR1. Continue

Vesuvius

ICP-MS trace elements data: Actlabs Ontario (Canada)

Sample name	ref.	Rb ppm	Sr ppm	Y ppm	Zr ppm	Nb ppm	Cs ppm	Ba ppm	La ppm	Ce ppm	Pr ppm	Nd ppm	Sm ppm	Eu ppm	Gd ppm	Tb ppm	Dy ppm	Ho ppm	Er ppm	Tm ppm	Yb ppm	Lu ppm	Hf ppm	Ta ppm	Pb ppm	Th ppm	U ppm
VES 01	this study	302	1037	27.4	190	31.9	18.5	2171	44.8	94	11.3	42.3	9.61	2.44	7.70	1.06	5.48	0.93	2.47	0.35	2.24	0.31	4.7	1.66	21	18.4	5.50
VES 02	this study	293	937	27.1	210	30.7	20.0	1997	47.9	101	12.5	47.0	10.5	2.66	8.32	1.08	5.44	0.92	2.50	0.34	2.17	0.31	5.3	1.62	33	21.9	6.82
VES 05	this study	314	1012	27.8	212	32.2	20.8	2137	49.1	105	12.6	46.6	10.4	2.63	8.28	1.10	5.44	0.92	2.49	0.35	2.21	0.32	5.2	1.70	29	22.0	6.78
VES 06	this study	280	1040	28.7	221	33.2	17.7	2087	49.5	107	13.0	49.6	10.9	2.75	8.95	1.11	5.73	0.96	2.53	0.36	2.27	0.32	5.5	1.76	12	21.9	6.61
VES 07	this study	331	1013	29.5	214	33.9	23.0	2107	47.2	101	12.5	46.6	10.1	2.56	8.22	1.08	5.33	0.91	2.47	0.35	2.08	0.32	5.3	1.69	30	22.1	7.11
VES 09	this study	336	1158	26.1	207	31.6	19.0	2352	52.2	106	12.5	45.4	9.4	2.36	7.28	1.02	5.05	0.89	2.33	0.33	2.03	0.30	4.7	1.81	44	21.8	6.73
VES 11	this study	259	974	26.7	198	28.6	16.7	2285	52.9	116	14.0	51.1	11.2	2.85	8.70	1.13	5.48	0.92	2.35	0.33	2.10	0.31	4.7	1.63	23	21.8	6.12
VES 16	this study	225	964	26.1	187	25.6	13.0	2214	44.0	93	11.5	44.5	10.1	2.51	7.46	1.10	5.29	0.96	2.54	0.36	2.24	0.33	4.7	1.51	27	16.5	6.04
VES 17	*Avanzinelli et al., 2008*	*307*	*885*	*22.5*	*206*	*40.0*	*17.5*	*2090*	*51.3*	*102*	*12.5*	*47.1*	*9.40*	*2.37*	*7.76*	*0.85*	*4.25*	*0.75*	*2.13*	*0.26*	*1.90*	*0.25*	*4.0*	*1.90*	*	*20.4*	*5.99*
VES 18	*Avanzinelli et al., 2008*	*278*	*941*	*21.0*	*182*	*32.0*	*15.8*	*2440*	*50.6*	*99*	*11.7*	*42.2*	*8.30*	*2.20*	*6.98*	*0.78*	*3.99*	*0.75*	*2.06*	*0.27*	*1.80*	*0.25*	*4.0*	*1.50*	*	*20.7*	*5.94*
95VS131	*Avanzinelli et al., 2008*	*290*	*933*	*24.7*	*185*	*33.0*	*16.2*	*2290*	*46.6*	*93*	*11.7*	*45.0*	*9.10*	*2.39*	*8.24*	*0.93*	*5.00*	*0.87*	*2.44*	*0.33*	*2.20*	*0.28*	*4.0*	*1.70*	*	*21.8*	*7.35*
97VS718b	*Avanzinelli et al., 2008*	*227*	*694*	*21.9*	*180*	*32.0*	*12.2*	*1710*	*46.0*	*94*	*11.7*	*45.3*	*9.50*	*2.27*	*8.20*	*0.92*	*4.23*	*0.77*	*2.20*	*0.25*	*1.90*	*0.26*	*4.0*	*1.60*	*	*18.7*	*6.07*
95VS135	*Avanzinelli et al., 2008*	*266*	*1050*	*24.1*	*210*	*33.0*	*13.0*	*2630*	*52.6*	*104*	*12.6*	*46.6*	*9.30*	*2.49*	*8.16*	*0.90*	*4.50*	*0.80*	*2.29*	*0.29*	*2.20*	*0.28*	*4.0*	*1.60*	*	*18.7*	*6.74*

Sediments

ICP-MS trace elements data: new data performed at Bristol Isotope Group (BIG)

Sample name	ref	Rb ppm	Sr ppm	Y ppm	Zr ppm	Nb ppm	Cs ppm	Ba ppm	La ppm	Ce ppm	Pr ppm	Nd ppm	Sm ppm	Eu ppm	Gd ppm	Tb ppm	Dy ppm	Ho ppm	Er ppm	Tm ppm	Yb ppm	Lu ppm	Hf ppm	Ta ppm	Pb ppm	Th ppm	U ppm
SD 11	this study	72.2	229	24.0	203	12.8	*	382	21.5	43	5.46	18.9	4.10	1.23	3.86	0.86	2.81	0.79	1.70	0.49	1.52	0.48	*	0.17	11	10.4	2.95
SD 48	this study	42.6	867	20.0	45	2.04	*	188	20.4	24	4.46	17.3	3.54	0.92	3.77	0.58	3.21	0.67	2.00	0.27	1.72	0.27	*	0.11	5	3.89	1.51
ERN57	*Boari et al., 2009*	*15.0*	*386*	*4.50*	*10*	*1.62*	*0.6*	*56.0*	*4.30*	*7*	*0.97*	*3.84*	*0.78*	*0.19*	*0.84*	*0.13*	*0.72*	*0.15*	*0.42*	*0.06*	*0.36*	*0.06*	*0.34*	*0.10*	*0.2*	*1.00*	*2.26*

Quality Control: *Meas/Ref is the ratio between the measured concentration value and the certified one of a number (n) of rock standards measured together with the samples*

	Rb	Sr	Y	Zr	Nb	Cs	Ba	La	Ce	Pr	Nd	Sm	Eu	Gd	Tb	Dy	Ho	Er	Tm	Yb	Lu	Hf	Ta	Pb	Th	U
Meas/Cert	*0.97*	*0.98*	*0.97*	*0.94*	*0.95*	*0.98*	*0.97*	*0.99*	*1.00*	*0.98*	*0.98*	*1.00*	*0.96*	*0.99*	*1.02*	*0.98*	*0.99*	*0.98*	*0.99*	*0.98*	*0.98*	*0.98*	*0.93*	*0.91*	*1.02*	*1.00*
1 σ	*0.04*	*0.03*	*0.10*	*0.06*	*0.13*	*0.05*	*0.06*	*0.08*	*0.04*	*0.12*	*0.04*	*0.04*	*0.08*	*0.07*	*0.11*	*0.07*	*0.05*	*0.09*	*0.07*	*0.06*	*0.05*	*0.10*	*0.15*	*0.33*	*0.07*	*0.08*
#	*14*	*12*	*19*	*11*	*15*	*16*	*12*	*28*	*26*	*18*	*31*	*29*	*32*	*18*	*24*	*23*	*20*	*20*	*23*	*32*	*25*	*17*	*19*	*14*	*25*	*23*

Table DR2. Sr and Nd isotopic composition of the studied samples and international standards

Vesuvius

	Eruption date	reference	Instrument-Laboratory	$^{87}Sr/^{86}Sr$	2 s.e.	$^{143}Nd/^{144}Nd$	2 s.e.
VES 01	1697 A.D.	this study	TIMS-UniFi	0.707311	0.000005	*0.512478*	0.000004
VES 02	1794 A.D.	this study	TIMS-UniFi	0.707685	0.000006	*0.512459*	0.000005
VES 05	1861 A.D.	this study	TIMS-UniFi	0.707614	0.000007	*0.512461*	0.000005
VES 06	1861 A.D.	this study	TIMS-UniFi	0.707436	0.000007	*0.512470*	0.000005
VES 07	1737 A.D.	this study	TIMS-UniFi	0.707617	0.000007	*0.512465*	0.000005
VES 09	1760 A.D.	this study	TIMS-UniFi	0.707267	0.000007	*0.512482*	0.000005
VES 11	1754 A.D.	this study	TIMS-UniFi	0.707944	0.000007	*0.512448*	0.000005
VES 16	1929 A.D.	this study	TIMS-UniFi	0.707190	0.000008	*0.512472*	0.000004
VES 17	1944 A.D	*Avanzinelli et al., 2008*	*TIMS-UniFi*	*0.707228*	*0.000005*	*0.512474*	*0.000006*
VES 18	1858 A.D.	*Avanzinelli et al., 2008*	*TIMS-UniFi*	*0.707437*	*0.000009*	*0.512462*	*0.000004*
95VS131	472-1631 A.D.			*	*	*	*
97VS718b	472-1631 A.D.	*Avanzinelli et al., 2008*	*TIMS-UniFi*	*0.707729*	*0.000009*	*0.512458*	*0.000005*
95VS135	472-1631 A.D.	*Avanzinelli et al., 2008*	*TIMS-UniFi*	*0.707325*	*0.000007*	*0.512477*	*0.000006*

Sediments

	lithology	reference	Instrument-Laboratory	$^{87}Sr/^{86}Sr$	2 s.e.	$^{143}Nd/^{144}Nd$	2 s.e.
SD 11	Carbonate-poor marlstone	this study	TIMS-UniFi	0.710361	0.000005	*0.512205*	0.000005
SD 48	Carbonate-rich marlstone	this study	TIMS-UniFi	0.708040	0.000005	*0.512163*	0.000005
ERN57	Mesozoic Limestone	*Boari et al., 2009*	*TIMS-UniFi*	*0.708841*	*0.000007*	*0.512151*	*0.000004*

Reproducibility of International Standards	$^{87}Sr/^{86}Sr$ measured	2 σ abs.	#
SRM 987 - within run analyses	0.710247	0.000008	*4*
SRM 987 - long term reproducibility	0.710248	0.000016	*108*
SRM 987 reference value (Thirlwall, 1991)	*0.710248*	*0.000011*	*427*
AGV1 standard	0.703982	0.000021	*5*
AGV1 reference value (Weis et al., 2006)	0.703996	0.000020	*10*

Reproducibility of International Standards	$^{143}Nd/^{144}Nd$	2 σ abs.	#
Nd-Fi (internal standard) within run analyses	0.511467	0.000004	7
Nd-Fi long term reproducibility	0.511467	0.000007	111
La Jolla long term reproducibility	0.511846	0.000007	67
La Jolla reference value (Thirlwall, 1991)	*0.511856*	*0.000007*	*44*

Sr and Nd isotopes were measured at the Radiogenic Isotopes Laboratory of the University of Firenze (Avanzinelli et al., 2005) with a Thermo Finnigan Triton Thermal Ionisation Mass Spectrometer (TIMS-UniFi) in multi-dynamic mode (Thirlwall, 1991). Internal errors on sample data (± 2 s.e.) are fully propagated for all the corrections applied. Reproducibility of International Standards is expressed as 2σ; (#) = number of analyses. Numbers in Italic are from Avanzinelli et al. (2008).

Table DR3. Pb isotopic composition of the studied samples and international standards

Vesuvius

	Eruption date	reference	Instrument-Laboratory	$^{206}Pb/^{204}Pb$ initial	2 s.e.	$^{207}Pb/^{204}Pb$ initial	2 s.e.	$^{208}Pb/^{204}Pb$ initial	2 s.e.
VES 01	1697 A.D.	this study	MC-ICPMS - BIG	19.079	0.008	15.692	0.005	39.189	0.017
VES 02	1794 A.D.	this study	MC-ICPMS - BIG	18.982	0.008	15.694	0.005	39.126	0.017
VES 05	1861 A.D.	this study	MC-ICPMS - BIG	19.010	0.008	15.684	0.005	39.120	0.017
VES 06	1861 A.D.	this study	MC-ICPMS - BIG	19.026	0.008	15.700	0.005	39.173	0.017
VES 07	1737 A.D.	this study	MC-ICPMS - BIG	19.009	0.008	15.688	0.005	39.131	0.017
VES 09	1760 A.D.	this study	MC-ICPMS - BIG	19.043	0.008	15.685	0.005	39.165	0.017
VES 11	1754 A.D.	this study	MC-ICPMS - BIG	18.961	0.007	15.689	0.005	39.122	0.017
VES 16	1929 A.D.	this study	MC-ICPMS - BIG	19.115	0.008	15.691	0.005	39.212	0.017
VES 17	1944 A.D	this study	MC-ICPMS - BIG	19.021	0.008	15.696	0.005	39.151	0.017
VES 18	1858 A.D.	this study	MC-ICPMS - BIG	19.080	0.008	15.695	0.005	39.195	0.017
95VS131	472-1631 A.D.	this study	MC-ICPMS - BIG	19.007	0.008	15.698	0.005	39.158	0.017
97VS718b	472-1631 A.D.	this study	MC-ICPMS - BIG	18.912	0.007	15.685	0.005	39.050	0.017
95VS135	472-1631 A.D.	this study	MC-ICPMS - BIG	19.078	0.008	15.696	0.005	39.191	0.017

Sediments

	lithology	reference	Instrument-Laboratory						
SD 11	Carbonate-poor marlstone	this study	TIMS-UniFi	18.851	0.013	15.679	0.015	38.910	0.056
SD 48	Carbonate-rich marlstone	this study	TIMS-UniFi	18.864	0.013	15.675	0.003	38.908	0.056

Reproducibility of International Standards		$^{206}Pb/^{204}Pb$ measured	2 σ abs.	$^{207}Pb/^{204}Pb$ measured	2 σ abs.	$^{208}Pb/^{204}Pb$ measured	2 σ abs.	#
SRM 982 (BIG) - long term reproducibility	MC-ICPMS - BIG	36.755	0.015	17.166	0.006	36.754	0.016	23
SRM 982 reference value (Baker et al., 2004)	*MC-ICPMS - double spike*	*36.743*		*17.162*		*36.749*		
BCR 2 (BIG)	MC-ICPMS - BIG	18.753	0.015	15.629	0.009	38.744	0.035	8
BCR 2 (UniFi)	TIMS-UniFi	18.749	0.003	15.618	0.003	38.714	0.011	7
BCR 2 reference value (Weis et al., 2006)	*MC-ICPMS - Tl correction*	*18.753*	*0.002*	*15.625*	*0.004*	*38.724*	*0.041*	*11*
BCR 2 reference value (Baker et al., 2004)	*MC-ICPMS - double spike*	*18.765*	*0.011*	*15.628*	*0.005*	*38.752*	*0.022*	*8*
BHVO 2 (BIG)	MC-ICPMS - BIG	18.641	0.012	15.532	0.044	38.242	0.037	10
BHVO 2 reference value (Weis et al., 2006)	*MC-ICPMS - Tl correction*	*18.647*	*0.024*	*15.533*	*0.009*	*38.237*	*0.018*	*5*
BHVO 2 reference value (Baker et al., 2004)	*MC-ICPMS - double spike*	*18.649*	*0.019*	*15.540*	*0.015*	*38.249*	*0.022*	*5*
AGV 1 (UniFi)	TIMS-UniFi	18.941	0.013	15.654	0.015	38.566	0.056	11
AGV 1 reference value (Weis et al., 2006)	*MC-ICPMS - Tl correction*	*18.940*	*0.006*	*15.653*	*0.004*	*38.560*	*0.010*	*5*
AGV 1 reference value (Baker et al., 2004)	*MC-ICPMS - double spike*	*18.942*	*0.002*	*15.658*	*0.002*	*38.569*	*0.006*	*12*

Pb isotope ratios of Vesuvius volcanic products were measured at BIG via Thermo-Finnigan Neptune MC-ICPMS. Instrumental mass fractionation was corrected by the average of the bracketing NIST SRM 981 run before and after the sample (Avanzinelli et al., 2014). Pb isotope ratios of the sediment samples were measured at the Radiogenic Isotopes Laboratory of the University of Firenze (i.e., UniFi) with a Thermo Finnigan Triton Thermal Ionisation Mass Spectrometer (TIMS). Mass bias was corrected by replicate analyses of NIST SRM 981 as described in Avanzinelli et al., 2005. The reproducibility of the international rock standards is expressed as 2 sigma (2σ): # = number of analyses. The internal errors (± 2 s.e.) on the samples' ratio are calculated from the reproducibility of SRM982 (for BIG measurements) and AGV 1 standards (UniFi), respectively. Reference values (Baker et al., 2004; Weis et al., 2006) adopted different protocols for mass-bias corrections using $^{205}Tl/^{203}Tl$ (Weis et al., 2006) and a $^{207}Pb/^{205}Pb$ double-spike (Baker et al., 2004), respectively.

Table DR4. U-series and $\delta^{238}U$ of the studied samples and international standards

Vesuvius

sample	Eruption date	reference	Instrument-Laboratory	U ppm	2 s.e.	Th ppm	2 s.e.	$(^{234}U/^{238}U)$	2 s.e.	$(^{238}U/^{232}Th)$	2 s.e.	$(^{230}Th/^{232}Th)$	2 s.e.	$(^{230}Th/^{238}U)$	2 s.e.		$\delta^{238}U$ ‰	2 s.e.
VES 01	1697 A.D.	this study	MC-ICPMS - BIG	5.747	0.027	16.963	0.089	1.001	0.002	1.028	0.008	0.897	0.002	0.872	0.003	**VES 01**	-0.30	0.02
rep		*this study*		*5.744*	*0.028*	*17.029*	*0.081*	*1.003*	*0.002*	*1.024*	*0.008*	*0.886*	*0.003*	*0.866*	*0.003*	*rep.*	*-0.22*	*0.06*
rep-2		*this study*		*6.540*	*0.019*	*19.187*	*0.065*	*0.999*	*0.002*	*1.034*	*0.005*	*0.890*	*0.002*	*0.861*	*0.003*			
VES 02	1794 A.D.	this study	MC-ICPMS - BIG	7.070	0.030	19.818	0.089	1.009	0.002	1.082	0.008	0.871	0.003	0.805	0.003			
rep		*this study*		*7.430*	*0.022*	*20.841*	*0.315*	*1.006*	*0.002*	*1.082*	*0.018*	*0.877*	*0.002*	*0.811*	*0.014*			
rep-2		*this study*		*7.101*	*0.024*	*19.731*	*0.074*	*0.999*	*0.001*	*1.092*	*0.006*	*0.868*	*0.003*	*0.795*	*0.003*			
VES 05	1861 A.D.	this study	MC-ICPMS - BIG	7.070	0.020	20.289	0.058	1.003	0.002	1.057	0.006	0.873	0.004	0.825	0.004			
rep		*this study*		*7.067*	*0.026*	*20.170*	*0.077*	*0.996*	*0.002*	*1.063*	*0.007*	*0.871*	*0.003*	*0.819*	*0.004*			
VES 06	1861 A.D.	this study	MC-ICPMS - BIG	6.962	0.034	20.203	0.091	0.998	0.002	1.046	0.007	0.886	0.002	0.847	0.003			
rep		*this study*		*6.332*	*0.019*	*18.487*	*0.056*	*1.003*	*0.002*	*1.039*	*0.005*	*0.885*	*0.002*	*0.851*	*0.003*			
VES 07	1737 A.D.	this study	MC-ICPMS - BIG	7.245	0.031	20.303	0.088	1.001	0.002	1.083	0.005	0.874	0.000	0.807	0.000	**VES 07**	-0.27	0.03
rep		*this study*		*7.175*	*0.024*	*20.256*	*0.069*	*1.002*	*0.002*	*1.075*	*0.006*	*0.869*	*0.003*	*0.809*	*0.003*			
VES 09	1760 A.D.	this study	MC-ICPMS - BIG	7.250	0.032	20.519	0.095	1.002	0.001	1.072	0.008	0.921	0.002	0.859	0.003			
rep		*this study*		*7.017*	*0.019*	*19.879*	*0.071*	*1.004*	*0.002*	*1.071*	*0.005*	*0.899*	*0.002*	*0.839*	*0.003*			
VES 11	1754 A.D.	this study	MC-ICPMS - BIG	6.498	0.029	20.454	0.088	0.994	0.002	0.964	0.007	0.850	0.003	0.882	0.004			
rep		*this study*		*5.840*	*0.017*	*18.342*	*0.060*	*1.003*	*0.002*	*0.966*	*0.005*	*0.852*	*0.002*	*0.882*	*0.003*			
VES 16	1929 A.D.	this study	MC-ICPMS - BIG	4.659	0.022	15.489	0.068	1.003	0.002	0.913	0.004	0.881	0.002	0.965	0.004	**VES 16**	-0.26	0.04
rep		*this study*		*4.668*	*0.016*	*15.777*	*0.058*	*0.999*	*0.002*	*0.898*	*0.005*	*0.865*	*0.002*	*0.963*	*0.004*			
VES 17	1944 A.D	this study	MC-ICPMS - BIG	6.293	0.025	19.096	0.077	1.001	0.002	1.000	0.007	0.874	0.003	0.874	0.004	**VES 17**	-0.29	0.02
rep		*this study*		*6.266*	*0.023*	*19.057*	*0.078*	*1.002*	*0.002*	*0.998*	*0.007*	*0.874*	*0.004*	*0.876*	*0.005*	*rep.*	*-0.31*	*0.05*
published		*Avanzinelli et al., 2008*		*6.30*		*19.45*		*1.001*	*0.003*	*0.983*	*0.005*	*0.868*	*0.005*	*0.884*	*0.004*			
VES 18	1858 A.D.	this study	MC-ICPMS - BIG	6.456	0.024	20.221	0.076	1.000	0.002	0.969	0.006	0.891	0.003	0.920	0.004	**VES 18**	-0.12	0.04
rep		*this study*		*6.412*	*0.026*	*20.048*	*0.089*	*1.001*	*0.002*	*0.970*	*0.007*	*0.886*	*0.004*	*0.913*	*0.004*			
rep-2		*this study*		*6.324*	*0.023*	*19.981*	*0.087*	*1.000*	*0.002*	*0.960*	*0.006*	*0.880*	*0.003*	*0.916*	*0.004*			
published		*Avanzinelli et al., 2008*		*6.340*		*20.170*		*1.001*	*0.003*	*0.953*	*0.004*	*0.878*	*0.005*	*0.921*	*0.003*			
95VS131	472-1631 A.D.	this study	MC-ICPMS - BIG	7.631	0.038	20.892	0.108	1.001	0.002	1.108	0.008	0.904	0.002	0.816	0.003			
published		*Avanzinelli et al., 2008*		*7.600*		*20.780*		*1.003*	*0.004*	*1.112*	*0.006*	*0.896*	*0.005*	*0.806*	*0.003*			
97VS718b	472-1631 A.D.	this study	MC-ICPMS - BIG	6.214	0.031	17.524	0.084	1.003	0.002	1.076	0.008	0.881	0.003	0.819	0.003	**97VS718b**	-0.19	0.04
published		*Avanzinelli et al., 2008*		*6.230*		*17.490*		*1.002*	*0.004*	*1.083*	*0.005*	*0.882*	*0.006*	*0.815*	*0.003*			
95VS135	472-1631 A.D.	this study	MC-ICPMS - BIG	6.696	0.030	16.778	0.080	1.001	0.002	1.211	0.008	0.890	0.002	0.735	0.002	**95VS135**	-0.24	0.04
published		*Avanzinelli et al., 2008*		*6.700*		*16.760*		*0.999*	*0.003*	*1.215*	*0.006*	*0.887*	*0.005*	*0.728*	*0.003*			

Sediments

					$\delta^{238}U$	2 s.e.
SD 11	Carbonate-poor marlstone	this study	MC-ICPMS - BIG	**SD 11**	-0.08	0.02
SD 48	Carbonate-rich marlstone	this study	MC-ICPMS - BIG	**SD 48**	0.19	0.06
ERN 57	Mesozoic Limestone	this study	MC-ICPMS - BIG	**ERN 57**	-0.67	0.04
				rep	*-0.68*	*0.03*

Reproducibility of International Standards

	U	2σ (#)	Th	2σ (#)	$(^{234}U/^{238}U)$	2σ (#)	$(^{238}U/^{232}Th)$	2σ (#)	$(^{230}Th/^{232}Th)_i$	2σ (#)	$(^{230}Th/^{238}U)_i$	2σ (#)		$\delta^{238}U$	2σ (#)
BCR 2	1.693	0.027 (17)	5.885	0.105 (17)	1.002	0.006 (17)	0.873	0.006 (17)	0.877	0.006 (17)	1.005	0.006 (17)	**BCR 2**	-0.280	0.028 (2)
TML	10.51	0.20 (23)	29.78	0.77 (23)	1.000	0.004 (23)	1.071	0.012 (23)	1.072	0.013 (23)	1.001	0.009 (23)			
CZ 1													**CZ 1**	-0.045	0.037 (8)
JB 2													**JB 2**	-0.313	0.076 (3)
BHVO 2													**BHVO 2**	-0.313	0.093 (4)

^{238}U-^{230}Th disequilibria were measured by isotoptope dilution using established techniques (Hoffmann et al., 2007; Avanzinelli et al., 2014) at BIG via MC-ICPMS by bracketing each sample between two standards, U112a for U measurements and an internal Th-standard for Th analyses. The possible influence of weathering or seawater alteration was checked by measuring ($^{234}U/^{238}U$) of the samples, all of which resulted within error of secular equilibrium values. Th and U contents are ppm. Parentheses denote isotope ratios are expressed as activity. Internal errors on sample data (± 2 s.e.) are fully propagated for all the corrections applied. Age corrections have not been applied due to the historic age of all the samples. Reproducibility of International Standards is expressed as 2σ; (#) = number of analyses. Replicates (in italic) are made on completely separate sample dissolutions. Published data performed on some of the same samples (Avanzinelli et al., 2008) are also reported. Accuracy and reproducibility was tested over the measurement period by several replicates of International standards BCR 2 and TML, all yielding values indistinguishable from secular equilibrium.

$^{238}U/^{235}U$ was measured via MC-ICPMS at BIG according to the procedure described in Andersen et al. (2014, 2015) using the IRMM-3636 ^{233}U-^{236}U double spike. A two-step sample purification procedure by TRU Resin chemistry allowed full U recovery (>85 %) and total chemistry blanks of 25 pg for all samples (negligible comparing with sample sizes). Measurements of unknown samples were bracketed and normalised to the CRM 145 standard that had been previously spiked. The mass bias corrected $^{238}U/^{235}U$ ratios were reported to δ-notation using the $^{238}U/^{235}U$ = 137.829 (±0.022) CRM 145 value (Hiess et al., 2012). The $\delta^{238}U$ was then normalised to the bracketed standard values measured along with the samples.

Table DR5. Trace element and isotope composition of the end-members used to model the mantle source of the Vesuvius magmas

Step I - Mantle prior to the addition of the U-rich Marl Melt Component		**Sr**	**Nd**	**Th**	**U**	**($^{238}U/^{232}Th$)**	**($^{230}Th/^{232}Th$)**	**($^{230}Th/^{238}U$)**	**$^{87}Sr/^{86}Sr$**	**$^{143}Nd/^{144}Nd$**	**$\delta^{238}U$**
		ppm	ppm	ppm	ppm						‰
Original mantle wedge (MW) (Tommasini et al., 2007)		22	1.2	0.06	0.02	1.01	1.01	1.00	0.703000	0.513090	-0.33
Slab derived component (SC) (Tommasini et al., 2007)		1172	59.6	24.00	6.55	0.83	0.83	1.00	0.709295	0.512145	-0.33
	% SC added										
Enriched mantle wedge beneath Vesuvius after Step I	3.5%	62	3.2	0.90	0.25	0.84	0.84	1.00	0.707148	0.51248	-0.33
Step II - U-rich Marl Melt Component (MMC)		**Sr**	**Nd**	**Th**	**U**	**($^{238}U/^{232}Th$)**	**($^{230}Th/^{232}Th$)**	**($^{230}Th/^{238}U$)**	**$^{87}Sr/^{86}Sr$**	**$^{143}Nd/^{144}Nd$**	**$\delta^{238}U$**
Starting materials											
Starting Sed 1. SD48 - High Carbonate marl		867	17.3	3.90	1.74	1.35	1.35	1.00	0.708040	0.512163	0.19
Starting Sed 2. SD11 - Low Carbonate marl		229	18.9	10.40	3.68	1.07	1.07	1.00	0.710360	0.512205	-0.08
Enrichment factors (Skora et al., 2015)	**run conditions**										
High carbonate	900°C, 25 % H_2O	1	0.03	0.05	0.95						
Low carbonate	850°C, 22 % H_2O	1	0.05	0.10	1.24						
Marl Melt Component (MMC)											
Melt from SD48 - High Carbonate (HC melt)		461	0.58	0.21	1.65	24.0	1.35	0.06	0.708040	0.512163	0.19
Melt from SD11 - Low Carbonate (LC melt)		279	0.91	1.02	4.57	13.7	1.07	0.08	0.710360	0.512205	-0.08
	% MMC added	**Sr**	**Nd**	**Th**	**U**	**($^{238}U/^{232}Th$)**	**($^{230}Th/^{232}Th$)**	**($^{230}Th/^{238}U$)**	**$^{87}Sr/^{86}Sr$**	**$^{143}Nd/^{144}Nd$**	**$\delta^{238}U$**
calculated average composition of Vesuvius mantle source (AD 1700 - AD 1944)	2.5 % of HC melt	72	3.18	0.88	0.28	1.03	0.88	0.86	0.707290	0.512481	-0.25
	1.0 % of LC melt	64	3.20	0.90	0.29	0.98	0.84	0.86	0.70729	0.51248	-0.29
BOC-derived fluid component (Avanzinelli et al., 2012; Andersen et al., 2015)		*203*	*2.8*	*0.07*	*0.16*	*6.7*	*1.09*	*0.16*			*-0.17*

The slab derived components used for Step I (from Tommasini et al., 2007) are assumed in secular equilibrium and their $\delta^{238}U$ is assumed equal to the bulk earth values reported in (Andersen et al., 2015). The Sr, Nd, U and Th contents of the BOC-derived fluids (used in Figs. 2 and DR2) are from (Avanzinelli et al., 2012) and its $\delta^{238}U$ is the average BOC value reported in Andersen et al., 2015). The paper of Skora et al., 2015 does not provide partition coefficients, but rather enrichment factors (i.e., the composition of the melt generated ratioed to that of the stating material), hence utilising such enrichment factors we implicitly assume similar degree of melting.

Table DR6. Estimates of CO_2 content in the Marl Melt Component (MMC)

	144-16 HC carbonate-rich marl Skora et al., 2015	**SD 48** carbonate-rich marl this study	**144-38 LC** carbonate-poor marl Skora et al., 2015	**SD 11** carbonate-poor marl this study
Initial CO_2 (wt%)	16.2%	*18.2%*	6.1%	*7.0%*
% residual $CaCO_3$	25.0%	*25.0%*	2.0%	*2.0%*
CO_2 in residual $CaCO_3$ (wt%[a])	11.0%	11.0%	0.9%	0.9%
CO_2 lost with melt (wt%[a])	5.2%	7.2%	5.2%	6.1%
% sed melt	58.0%	*58.0%*	66.0%	*66.0%*
CO_2 carried with sed. melt (wt%)	**9.0%**	**12.4%**	**7.9%**	**9.3%**

The amount of CO_2 retained in carbonate is calculated by stoichiometrically allotting it into the $CaCO_3$ formula. Numbers in Italic are estimated assuming similar CO_2/LOI and phase proportions of the HC and LC sediments reported in Skora et al. (2015). [a] : The % values are referred to the bulk initial marl. The remaining CO_2 has been redistributed into melt in order to provide an estimate of the CO_2 contents carried along wih it. See the Data Repository for further explanations.

Table DR7. Parameters used for CO_2 flux calculations

Period of activity	AD 1697- AD 1944		
Variable parameters	**example HC-marl addition**	**range for Monte Carlo simulations**	**source**
% of marl melt added: %MMC	2.5%	1.0 - 2.5%	Mixing model (Table DR5)
mean [U] of Vesuvius mantle source : $[U]_{MS}$	0.28 ppm	0.28 -0.29 ppm	Mixing model (Table DR5)
Vesuvius Output/Supply Rate (volume/year)	3.5×10^6 m^3/yr	$3.0 - 4.0 \times 10^6$ m^3/yr	Cortini and Scandone (1982); Scandone et al. (1986); Santacroce et al. (1993); Scandone et al. (2008)
$[U]_{ER}$	6.5 ppm	5.7 - 7.2 ppm	Our dataset and GeoRoc database
$[CO_2]_{MMC}$	10 wt%	8 - 13 wt%	Table DR6
Calculated masses and fluxes			
$OR_{1697-1944}$ *: Mass Output/Supply Rate:*	9.4 Mt/yr		
$fU_{ER} = fU_{MS}$ *: Uranium mass flux:*	61 t/yr		
f_{MS} *: Mass rate of mantle source undergoing meltinq:*	220 Mt/yr		
f_{MMC} *: Mass Flux of MMC:*	5.5 Mt/yr		
MMC-derived CO_2 flux: $f_{CO2-MMC}$	**0.55 Mt/yr**	*Fig. 3*	

The first column shows an example of the calculations made to obtain the estimate for the MMC-derived CO_2 fluxes (as describe in the Data Repository) considering a single set of parameters. The range used for the Monte Carlo simulations a are reported in the second comulm. Output rates values are considered as Dense Rock Equivalent (Santacroce et al., 1993). The mass of of magma erupted (in Mt=10^6 tons) are calcualted from the output rate a mean density of 2700 kg/m^3. See the Data Repository for further explanations.